

# Pose Stabilization of a Bar Tethered to Two Aerial Vehicles

Pedro O. Pereira<sup>a</sup>, Dimos V. Dimarogonas<sup>a</sup>

<sup>a</sup>*School of Electrical Engineering and Computer Science, KTH Royal Institute of Technology, SE-100 44, Stockholm, Sweden.*

---

## Abstract

This work focuses on the modeling, control and analysis of a bar, tethered to two unmanned aerial vehicles, which is required to stabilize around a desired pose. We follow a Newtonian approach when deriving the equations of motion, we close the loop by equipping each UAV with a PID control law, and finally we linearize the closed-loop vector field around some equilibrium points of interest. When requiring the bar to stay on the horizontal plane and under no normal stress, we verify that the bar's motion is decomposable into three decoupled motions, namely a longitudinal, a lateral and a vertical: for a symmetric system, each of those motions is further decomposed into two decoupled sub-motions, one linear and one angular; for an asymmetric system, we provide relations on the UAVs' gains that compensate for the system asymmetries and which decouple the linear sub-motions from the angular sub-motions. From this analysis, we provide conditions, based on the system's physical parameters, that describe *good* and *bad* types of asymmetries. Finally, when requiring the bar to pitch or to be under normal stress, we verify that there is a coupling between the longitudinal and the vertical motions, and that a positive normal stress (tension) has a positive effect on the stability, while a negative normal stress (compression) has a negative effect on the stability.

---

## 1. Introduction

Vertical take off and landing rotorcrafts, with hovering capabilities, provide a platform for transportation of cargos in dangerous and cluttered environments [1]. In cluttered environments, transportation with a single UAV may be the only feasible option, while transportation with multiple UAVs is primarily necessary when the cargo exceeds the individual UAVs' payload capacity. However, transportation with multiple UAVs is inevitable if one wishes to control the pose of the cargo: in particular, controlling the pose of a bar requires a minimum of two UAVs, while controlling the pose of a generic rigid body requires a minimum of three UAVs [2].

Using tethers in conjunction with UAVs can serve different and distinct purposes. Tethers/cables may be used to supply power or fuel to the UAV and thus to extend its flight time, or they may be used to provide an uninterrupted data transmission link [3–5]. However, in this paper, the purpose of the cables is to physically couple one or more UAVs to a cargo: when the cables are slack, the cargo is free of actuation; on the contrary, when they are taut, the cables provide an actuation medium for stabilizing the pose of the cargo. In this work, we assume that the cables are always taut, and thus that they behave as massless rigid links. A hybrid model, as in [6–8], can provide a more complete description of the dynamics of tethered transportation by accounting for the hybrid behaviour of the cables. However, the focus of this paper is

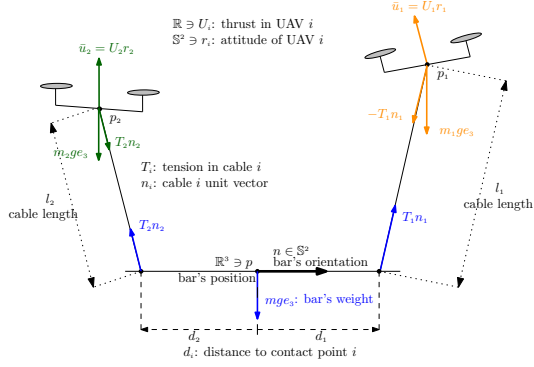
on the control design and analysis of the local closed-loop behavior, rendering a complete hybrid model of the system redundant.

Manipulator-endowed transportation [9–11] provides an alternative to tethered transportation. However, tethered transportation is mechanically simple and inexpensive, while robotic manipulators are heavy and therefore diminish the useful payload capacity a UAV can carry. Several control strategies for slung-load transportation, i.e., tethered transportation of a point-mass cargo by a single UAV, are found in the literature: the load swing can be dampened by appropriately planning trajectories, or by using vision and force measurements [12–16]; compensating for unknown model parameters can also be accomplished [17, 18]; and, when the point-mass cargo exceeds the allowed UAV's payload, cooperative tethered transportation becomes imperative [19–21].

This paper, on the other hand, focuses on transportation of a non-point-mass cargo. Control laws with an extended domain of operation and an extended domain of attraction are found in the literature [22–24], which can deal with asymmetries of the system but which lack experimental validation. On the other hand, cooperative transportation of rigid body cargos using simpler control laws has been tested and validated under various symmetry conditions (where UAVs are identical, cables are of the same length, and contact points are symmetrically distributed on the cargo) [2, 25–28]. We emphasize that aerial cooperative tethered transportation comes with multiple degrees of freedom, which can be exploited to, for example, minimize the internal forces applied on the cargo [29, 30]. In this manuscript, we focus on stabilization of a rod-like object tethered to two UAVs, as pictured in Fig. 1.

---

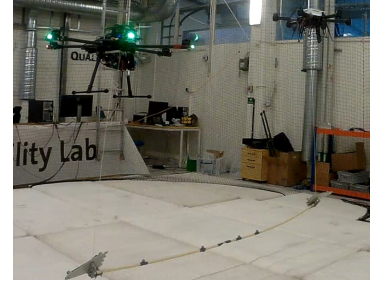
<sup>☆</sup>This work was supported by the EU H2020 Research and Innovation Programme under GA No.644128 (AEROWORKS), the Swedish Research Council (VR), the Swedish Foundation for Strategic Research (SSF) and the KAW Foundation.



(a) Modeling of the system (given the bar's orientation,  $d_1 > 0$  and  $d_2 < 0$ ).



(b) Symmetric system [31].



(c) Non-symmetric system [32].

Figure 1: Tethered transportation of a rod-like object by two aerial vehicles (in a symmetric system, the UAVs are identical, the cables are of the same length, and the contact points are equally distanced from the bar's center-of-mass).

This problem has also been considered in [26, 31–33]. In [33], a master-slave approach for the two UAVs is adopted, where the UAV slave estimates the cable force exerted on itself. In [26], vision is used to autonomously estimate the bar's pose. In [31, 32], relations on the UAVs' PID gains are provided for which stability – regarding the bar's pose stabilization – is guaranteed. We note that [26, 31–33] take the system to be symmetric and/or stabilize the bar on the horizontal plane and under no normal stress; whereas, in this paper, we relax both of these conditions. We perform an analysis similar to that in [6, 34, 35], where we linearize the system, and derive conditions on the gains that guarantee exponential stability regarding the stabilization of the bar's pose. We note that the state-space of the system is a manifold, and for that reason we provide an analysis tool that allows us to linearize the vector field around a point in the state-space without having to provide a parameterization of the manifold.

The results of this paper are partially based on [31, 32], with the first focusing on the symmetric case, and the second focusing on the asymmetric case. This paper's main contributions, which we list next, are also the distinguishing factors with respect to [31, 32]. (i) We provide a detailed model derivation of the system, based on a Newtonian approach, and we show that the open-loop vector field is invariant to translations and rotations around the vertical direction; we also describe and parametrize the open-loop equilibrium points and equilibrium inputs, from which we derive the necessity of integral action terms in the vertical direction of each UAVs' control law – Section 3. (ii) We construct a bounded PID-like control law, which guarantees that physical input limitations can be met, and that the desired UAVs' attitude are always well-defined; we then show that the closed-loop equilibria of interest are entirely parameterizable with just two parameters, namely the desired pitch angle of the bar ( $\theta_*$ ), and the desired normal stress to be exerted on the bar ( $F_*$ ) – Section 4. (iii) When  $(\theta_*, F_*) = (0, 0)$ , we show that the system's motion can be broken down into three decoupled motions (vertical, longitudinal and lateral), with each motion being

composed of two sub-motions (one linear and one angular) – Sections 6.3 and 6.4. When  $\theta_* \neq 0$  or  $F_* \neq 0$ , we show that the longitudinal and the vertical motions are no longer decoupled; we also find out that a bar under tension, as opposed to a bar under compression, is beneficial when it comes to stability – Sections 6.5 and 6.6. For all the different cases, we provide conditions on the control law PID gains that guarantee that each and every motion/sub-motion is asymptotically stable, and therefore that the equilibrium of the non-linear system is (locally) exponentially stable. We also provide conditions, based on the system's physical parameters, that describe *good* and *bad* types of asymmetries: e.g., it is better for the heavier vehicle to be attached to the shorter cable, in the sense that stability is guaranteed by a smaller proportional gain. All the derivations described in the paper may also be verified in the Mathematica notebook files found in [36].

## 2. Notation

The map  $\mathcal{S} : \mathbb{R}^3 \rightarrow \mathbb{R}^{3 \times 3}$  yields a skew-symmetric matrix and it satisfies  $\mathcal{S}(a)b = a \times b$ , for any  $a, b \in \mathbb{R}^3$ .  $\mathbb{S}^2 := \{x \in \mathbb{R}^3 : x^T x = 1\}$  denotes the set of unit vectors in  $\mathbb{R}^3$ . The map  $\Pi : \mathbb{S}^2 \ni x \mapsto \Pi(x) := I_3 - xx^T \in \mathbb{R}^{3 \times 3}$  yields a matrix that represents the projection onto the subspace orthogonal to  $x \in \mathbb{S}^2$ . We denote  $A_1 \oplus \dots \oplus A_n$  as the block diagonal matrix with block diagonal entries  $A_1$  to  $A_n$  (square matrices). Given some  $n, m \in \mathbb{N}$ , and a function  $f : \mathbb{R}^n \ni a \mapsto f(a) \in \mathbb{R}^m$ ,  $Df : \mathbb{R}^n \ni a \mapsto Df(a) \in \mathbb{R}^{m \times n}$  denotes the derivative of  $f$ . We denote by  $e_1, \dots, e_n \in \mathbb{R}^n$  the canonical basis vectors in  $\mathbb{R}^n$ .

## 3. Problem Description

Consider the system illustrated in Fig. 1a, with two VTOL aerial vehicles, a one dimensional bar and two cables connecting the aerial vehicles to distinct contact points on the bar. Fig. 1a provides a two-dimensional picture of the real system, as shown in Figs. 1b and 1c, but the modeling we describe next is three dimensional. Hereafter,

and for brevity, we refer to this system as UAVs-bar system. We denote by  $p_1, p_2, p \in \mathbb{R}^3$  and by  $v_1, v_2, v \in \mathbb{R}^3$  the UAVs' and the bar's center-of-mass positions and velocities; by  $n, \omega \in \mathbb{R}^3$  the bar's angular position (orientation) and angular velocity; and by  $r_1, r_2 \in \mathbb{S}^2$  the UAVs' thrust body directions. As for physical constants, we denote by  $m_1, m_2, m > 0$  the UAVs' and bar's masses; by  $J > 0$  the bar's moment of inertia (w.r.t. the bar's center-of-mass); by  $l_1, l_2 > 0$  the cables' lengths; and, finally, by  $d_1, d_2 \in \mathbb{R}$  the distance to the contact points on the bar at which the cables are attached to ( $d_i$  is positive if the contact point  $i$  is away from the bar's center-of-mass by a distance  $|d_i|$  and along the positive bar's direction, i.e., along  $+n \in \mathbb{S}^2$ ; and, it is negative if it is away from the bar's center-of-mass along the opposite direction, i.e., along  $-n \in \mathbb{S}^2$  – see Fig. 1a).

Finally, we denote by  $u_1, u_2 \in \mathbb{R}^3$  the input forces on the UAVs-bar system: for  $j \in \{1, 2\}$ ,  $\bar{u}_j := U_j r_j := u_j^T r_j r_j$  is the UAV's  $j$  input force, where the throttle  $U_j$  is taken as the inner product between the input  $u_j$  and the UAV's thrust direction  $r_j$  (one may think of  $u_j$  as the desired value for  $\bar{u}_j$ ).

Consider then the position variables  $z_p$ , the velocity variables  $z_v$ , the state  $z$ , and the input  $u$  defined as

$$z_p := (p, n, p_1, p_2) \in \mathbb{R}^{12}, z_v := (v, \omega, v_1, v_2) \in \mathbb{R}^{12}, \quad (1)$$

$$z := (z_p, z_v) \in \mathbb{R}^{24}, u := (u_1, u_2) \in \mathbb{R}^6. \quad (2)$$

Given the position and the velocity variables in (1), the system kinematics  $Z_p$  are given by

$$\dot{z}_p = Z_p(z) : \Leftrightarrow \dot{z}_p = \underbrace{(I_3 \oplus \mathcal{S}(-n) \oplus I_3 \oplus I_3)}_{=: \bar{Z}_p(z_p) \in \mathbb{R}^{12 \times 12}} z_v. \quad (3)$$

Consider now the map  $f : \mathbb{R}^{24} \rightarrow \mathbb{R}^6$ , which, when equal to  $0_6$ , encapsulates the constraints illustrated in Fig. 1a, defined as

$$f(z) := \begin{bmatrix} f_1(z_p) \\ f_2(z_p) \\ f_3(z_p, z_v) \\ f_4(z_p, z_v) \\ f_5(z_p) \\ f_6(z_p, z_v) \end{bmatrix} := \begin{bmatrix} l_1^{-2} \|p + d_1 n - p_1\|^2 - 1 \\ l_2^{-2} \|p + d_2 n - p_2\|^2 - 1 \\ Df_1(z_p) Z_p(z) \\ Df_2(z_p) Z_p(z) \\ n^T n - 1 \\ n^T \omega \end{bmatrix}. \quad (4)$$

Specifically, (the constraints' nomenclature we adopt here is the standard one; see, f.e., [37]):  $f_1$  and  $f_2$  are geometric constraints imposed by the cables, which require that the distance between each contact point on the bar and the corresponding UAV is equal to the corresponding cable length.  $f_3$  and  $f_4$  are kinematic (holonomic) constraints which follow from differentiation of the previous two geometric constraints.  $f_5$  is a geometric constraint which implies that the bar's angular position  $n$  is given by a unit vector<sup>1</sup>. And  $f_6$  is a kinematic (nonholonomic) constraint which implies that the bar's angular velocity  $\omega$  is orthogonal to the bar's angular position  $n$ , and thus that the bar does not rotate around itself.

<sup>1</sup>We do not need to include the kinematic (holonomic) constraint which follows from differentiation, since it is satisfied irrespectively of  $z$ : indeed,  $Df_5(z_p) \dot{z}_p(z) \stackrel{(3)}{=} 2n^T \mathcal{S}(\omega) n = 0$  for all  $n, \omega \in \mathbb{R}^3$ .

The necessity for specifying the constraints is two-fold. First, it allows us to define the state-space and the tangent set to each point in the state-space; this, in turn, will allow us to determine the tensions in each cable. Secondly, when linearizing the closed-loop vector field around the desired equilibrium, the constraints imposed by  $f$  in (4) play a crucial role in examining whether the Jacobian matrix is Hurwitz or not (see Section 6). Indeed, the constraints defined in (4) give rise to the state space and the corresponding tangent space given by

$$\mathbb{Z} := \{z \in \mathbb{R}^{24} : f(z) = 0_6\} \text{ and} \quad (5)$$

$$T_z \mathbb{Z} := \{\dot{z} \in \mathbb{R}^{24} : Df(z) \dot{z} = 0_6\}, \quad (6)$$

where  $\mathbb{Z}$  is a manifold of dimension  $18 = 24 - 6$ , and where we recall that  $Df(z) \in \mathbb{R}^{6 \times 24}$  is the derivative of  $f$  at  $z$ . Given an appropriate input  $u : \mathbb{R}_{\geq 0} \rightarrow \mathbb{R}^6$ , a system's trajectory  $z : \mathbb{R}_{\geq 0} \ni t \mapsto z(t) \in \mathbb{Z}$  evolves according to

$$\dot{z}(t) = Z(z(t), u(t)), z(0) \in \mathbb{Z}, \quad (7a)$$

where the vector field  $Z : \mathbb{Z} \times \mathbb{R}^6 \ni (z, u) \mapsto Z(z, u) \in \mathbb{R}^{24}$  is given by

$$\dot{z} = Z(z, u) : \Leftrightarrow \begin{bmatrix} \dot{z}_p \\ \dot{z}_v \end{bmatrix} = \begin{bmatrix} Z_p(z) \\ Z_v(z, u) \end{bmatrix}, \quad (7b)$$

with the kinematics  $Z_p$  defined in (3), and with the dynamics  $Z_v$  corresponding to the linear and the angular accelerations. The forces and their application points are depicted in Fig. 1a, which allows us to write down the dynamics  $Z_v$  of the system. For that purpose, and for convenience, consider the notations

$$n_i \equiv \frac{p_i - (p + d_i n)}{l_i} \in \mathbb{S}^2, \mathcal{T}_i \equiv T_i(z, u) n_i \in \mathbb{R}^3, \quad (8)$$

where  $n_i$  is the unit vector associated to the cable  $i$  (indeed,  $\frac{p_i - (p + d_i n)}{l_i} \in \mathbb{S}^2$  for all  $z \in \mathbb{Z}$  – see (4)); and where  $T_i(z, u)$  is the tension on cable  $i$  (which depends on the state  $z$  and the input  $u$ ).

Given the velocity variables, as introduced in (1), the dynamics are then given by (below,  $g$  stands for the acceleration due to gravity; and  $n_i$  is the shorthand in (8))

$$\dot{z}_v = Z_v(z, u) : \Leftrightarrow \quad (9)$$

$$\begin{bmatrix} \dot{v} \\ \dot{\omega} \\ \dot{v}_1 \\ \dot{v}_2 \end{bmatrix} = \underbrace{\begin{bmatrix} -ge_3 \\ 0_3 \\ \frac{u_1}{m_1} - ge_3 \\ \frac{u_2}{m_2} - ge_3 \end{bmatrix}}_{=: \mathcal{G}(u) \in \mathbb{R}^{12}} + \underbrace{\begin{bmatrix} \frac{n_1}{J} & \frac{n_2}{J} \\ d_1 \mathcal{S}(n) n_1 & d_2 \mathcal{S}(n) n_2 \\ -\frac{n_1}{m_1} & 0_3 \\ 0_3 & -\frac{n_2}{m_2} \end{bmatrix}}_{=: \mathcal{N}(z_p) \in \mathbb{R}^{12 \times 2}} \begin{bmatrix} T_1(z, u) \\ T_2(z, u) \end{bmatrix},$$

and where the tensions  $T_1(z, u), T_2(z, u)$  are described next (their expression is found in (11)). We emphasize that the tensions are internal forces – see Remark 1 – and therefore their expression must be found by exploring the constraints imposed on the system. Indeed, recall that the system is subject to the constraints in (4), which means that the state space  $\mathbb{Z}$  in (5) must be invariant with respect to the vector field  $Z$  in (7b), and, therefore, that

$$Z(z, u) \in T_z \mathbb{Z} \text{ for all } (z, u) \in \mathbb{Z} \times \mathbb{R}^6. \quad (10)$$

Combining (6) and (10), it follows that six constraints are imposed on the vector field  $Z$ . The satisfaction of the con-

$$\begin{bmatrix} \frac{d}{dt}f_3(z_p, z_v) \\ \frac{d}{dt}f_4(z_p, z_v) \end{bmatrix} = \begin{bmatrix} 0 \\ 0 \end{bmatrix} \Leftrightarrow \begin{bmatrix} T_1(z, u) \\ T_2(z, u) \end{bmatrix} = - \left( \begin{bmatrix} Df_1(z_p) \bar{Z}_p(z_p) \mathcal{N}(z_p) \\ Df_2(z_p) \bar{Z}_p(z_p) \mathcal{N}(z_p) \end{bmatrix} \right)^{-1} \left( \begin{bmatrix} D_1 f_3(z_p, z_v) Z_p(z) + Df_1(z_p) \bar{Z}_p(z_p) \mathcal{G}(u) \\ D_1 f_4(z_p, z_v) Z_p(z) + Df_2(z_p) \bar{Z}_p(z_p) \mathcal{G}(u) \end{bmatrix} \right). \quad (11)$$

straints that follow from the (three) geometric constraints is immediate (since these correspond to the kinematic holonomic constraints already included in (4)). The satisfaction of the constraint that follows from the non-holonomic kinematic constraint follows from the fact that  $\dot{\omega}$  in (9) is orthogonal to  $n$  ( $\frac{d}{dt}f_5(z_p, z_v) = \frac{d}{dt}n^T\omega = \dot{n}^T\omega + n^T\dot{\omega} = 0$ ). Finally, it remains to verify the satisfaction of the constraints that follow from the holonomic kinematic constraints: these constraints are those in (11), which completely define the tensions in the cables (the inverse in (11) is well-defined for all  $z_p$  [36]).

**Remark 1.** The tensions  $T_1(z, u), T_2(z, u) \in \mathbb{R}$ , in (9), are internal forces to the mechanical system, and, as such, they do not contribute to the change of linear and angular momentum of the system (see [36]).

**Remark 2.** The vector field  $Z$  in (7b) is input affine, that is  $\dot{z} = Z(z, u) \Leftrightarrow \dot{z} = A(z) + B(z_p)u$  for some  $A(z) \in \mathbb{R}^{24}$  and  $B(z_p) \in \mathbb{R}^{24 \times 6}$ .

### 3.1. Equilibria

In the previous section, we specified the vector field that describes the motion of our system, i.e.,  $\dot{z} = Z(z, u)$ . In this section, we specify the open-loop equilibria (non-exhaustive list however), i.e., given a constant input  $u \in \mathbb{R}^6$ , we determine the states  $z \in \mathbb{Z}$  for which  $0_{24} = Z(z, u)$ . The open-loop equilibria we describe next are illustrated in Fig. 2. As we verify next, in open-loop, there exists a continuum of equilibrium points, and therefore no such point is asymptotically stable. This provides the motivation for closing the loop, under an appropriate control law, which we specify in Section 4.

In what follows, let  $u \in \mathbb{R}^6$  be some constant input, for which we wish to determine the possible open-loop equilibria. The equilibria set is given by  $E_u := \{z \in \mathbb{Z} : Z(z, u) = 0_{24}\}$ , with  $Z$  as the vector field in (7b). It follows from the first six equations in (9) that (recall that the cables are connected to distinct contact points, i.e.,  $d_1 \neq d_2$ )

$$\begin{bmatrix} \dot{v} \\ \dot{\omega} \end{bmatrix} = \begin{bmatrix} 0_3 \\ 0_3 \end{bmatrix} \Leftrightarrow \begin{bmatrix} T_1 \\ T_2 \end{bmatrix} = \begin{bmatrix} \frac{d_2}{d_2-d_1}mge_3 + Fn \\ \frac{d_1}{d_1-d_2}mge_3 - Fn \end{bmatrix}, \quad (13a)$$

for any  $F \in \mathbb{R}$ , whose meaning will become clear next. It follows from the final six equations in (9) that

$$\begin{bmatrix} \dot{v}_1 \\ \dot{v}_2 \end{bmatrix} = \begin{bmatrix} 0_3 \\ 0_3 \end{bmatrix} \stackrel{(13a)}{\Leftrightarrow} \begin{bmatrix} u_1 \\ u_2 \end{bmatrix} = \begin{bmatrix} m_1ge_3 + \frac{d_2}{d_2-d_1}mge_3 + Fn \\ m_2ge_3 + \frac{d_1}{d_1-d_2}mge_3 - Fn \end{bmatrix} \quad (13b)$$

$$\Leftrightarrow \begin{bmatrix} (\delta_1 :=) u_1 + u_2 - (m_1 + m_2 + m)ge_3 \\ (\delta_2 :=) \frac{d_1(u_1 - m_1ge_3) + d_2(u_2 - m_2ge_3)}{d_1 - d_2} \end{bmatrix} = \begin{bmatrix} 0_3 \\ Fn \end{bmatrix}. \quad (13c)$$

That is, (13b) describes the conditions an input  $(u_1, u_2) \in \mathbb{R}^3 \times \mathbb{R}^3$  to sustain an equilibrium. (i) Each UAV needs to cancel its own weight (term  $m_i ge_3$  in (13b)). (ii) Each UAV needs to cancel some part of the bar's weight (term

$\frac{d_i}{d_j - d_i}mge_3$  in (13b)), and where the fraction of weight depends on the contact points on the bar. In particular, if  $d_1 = -d_2$ , then each UAV carries half of the bar's weight; on the other hand, if  $|d_i| \gg |d_j|$  then UAV  $j$  carries most of the bar's weight. (iii) One UAV applies some force  $F \in \mathbb{R}$  along the bar's angular position  $n$ , while the other applies an opposite force. For simplicity, let  $d_1 > 0$  and  $d_2 < 0$ : then, if the force  $F > 0$ , then the bar is under tension; if the force  $F < 0$ , then the bar is under compression; and finally, if  $F = 0$ , the bar is under no normal force/stress<sup>2</sup>.

**Remark 3.** Let  $F = 0$  in (13a). If  $d_1, d_2$  have opposite signs, then both cables are under tension. If  $d_1, d_2$  have the same sign, then the cable with the smallest  $|d_i|$  is under tension, and the one with the largest is under compression, which is not possible for a cable. For that reason, hereafter, we will assume that  $d_1$  and  $d_2$  have opposite signs.

**Proposition 4.** Let  $u \in \mathbb{R}^6 \Leftrightarrow (u_1, u_2) \in \mathbb{R}^3 \times \mathbb{R}^3$  be some chosen constant input, such that  $e_3^T u_1 > m_1 g$  and  $e_3^T u_2 > m_2 g$ . Denote  $E_u := \{z \in \mathbb{Z} : Z(z, u) = 0_{24}\} = \{z \in \mathbb{Z} : z_v = 0_{12} \text{ and } z_p = (p, n, p + d_1 n + l_1 n_1, p + d_2 n + l_2 n_2)\}$ , for some  $(p, n) \in \mathbb{R}^3 \times \mathbb{S}^2$  and some  $(n_1, n_2) \in \mathbb{S}^2 \times \mathbb{S}^2$ , as the equilibria set for the input  $u \in \mathbb{R}^6$ . Consider then  $\delta_1, \delta_2$  as defined in (13c). The following cases follow: (i) If  $\delta_1 \neq 0_3$ , then  $E_u$  is that above with  $(p, n) \in \emptyset$  (i.e.,  $E_u = \emptyset$ ). (ii) If  $\delta_1 = 0_3$  and  $\delta_2 = 0_3$ , then  $E_u$  is that above for any  $(p, n) \in \mathbb{R}^3 \times \mathbb{S}^2$  and with  $n_i = \frac{u_i - m_i ge_3}{\|u_i - m_i ge_3\|} \in \mathbb{S}^2$ . (iii) If  $\delta_1 = 0_3$  and  $\delta_2 \neq 0_3$ , then  $E_u$  is that above for any  $(p, n) \in \mathbb{R}^3 \times \{\pm \delta_2 / \|\delta_2\|\}$  and with  $n_i = \frac{u_i - m_i ge_3}{\|u_i - m_i ge_3\|} \in \mathbb{S}^2$ .

A proof is found in [36]. Proposition 4 provides some insight into the problem. Firstly, there are two non-binding conditions (inequalities), namely  $e_3^T u_1 > m_1 g$  and  $e_3^T u_2 > m_2 g$  which guarantee that, at the equilibrium, both cables are pointing up ( $e_3^T n_i = \frac{e_3^T u_i - m_i g}{\|u_i - m_i ge_3\|} > 0$ ). There are however three binding conditions (equalities), namely  $\delta_1 = 0_3 \Leftrightarrow u_1 + u_2 = (m_1 + m_2 + m)ge_3$ . It follows from the latter that  $e_3^T \delta_1 = 0 \Leftrightarrow e_3^T (u_1 + u_2) = (m_1 + m_2 + m)g$ , which states that the combined inputs need to compensate for the combined weight of the whole system. This binding condition on the inputs is hard to satisfy since one does not know exactly the weights of the UAVs and of the bar; in experiments, it is therefore important to include, on each UAV, an integrator in the vertical direction so that the latter binding condition can be satisfied. Two more binding conditions follow from  $\delta_1 = 0_3$ , namely  $e_1^T \delta_1 = 0$  and  $e_2^T \delta_1 = 0$ : when  $F = 0$  (no normal force applied on the bar), these conditions are met when  $e_1^T u_i = e_2^T u_i = 0$

<sup>2</sup>Let  $d_1 > 0$  and  $d_2 < 0$  and assume we are at the equilibrium, where (13a) holds: then the average normal force on the bar is given by  $2n^T \left( \frac{d_1}{d_1 - d_2} T_1 - \frac{d_2}{d_2 - d_1} T_2 \right) = 2F$  - see [36].

(no horizontal input from both UAVs), where the latter conditions are easy to satisfy (and the main reason for not including integrators in the horizontal components).

Proposition 4 also tells us that no equilibrium is asymptotically stable in open-loop, since  $E_u$  in (ii) and (iii) corresponds to a continuum of equilibrium points. However, when the condition  $\delta_2 \neq 0_3$  is satisfied, the equilibrium angular position of the bar (i.e.  $n$ ) is uniquely determined up to a sign: intuition suggests that one equilibrium attitude might be asymptotically stable – the one where the bar is under tension; while the diametrically opposed attitude might be unstable – the one where the bar is under compression. Based on the previous intuition, one might be tempted into trying to satisfy the condition  $\delta_2 \neq 0_3$  where the bar is under the normal force  $F \neq 0$ . There is however one disadvantage if this option is pursued: note from (13b) that both UAVs need to provide  $+Fn$  and  $-Fn$  respectively, which requires both synchrony and also accuracy. Since the controllers are distributed (i.e., one controller on each UAV), perfect synchrony is hard to accomplish. On the other hand, if the UAVs are heterogeneous, it is also hard to guarantee that one UAV provides  $+Fn$ , while the other provides  $-Fn$ . One possible solution to this problem is the inclusion of an integrator (on each of the UAVs' control law) along the bar's angular position.

In the experiments, only the scenario  $\delta_2 = 0_3 \Leftrightarrow F = 0$  has been tested, that is, the scenario where the bar is under no normal force at equilibrium. For this scenario (see (13b)), it follows that  $u_1 = m_1 g e_3 + \frac{d_2}{d_2 - d_1} m g e_3$  and that  $u_2 = m_2 g e_3 + \frac{d_1}{d_1 - d_2} m g e_3$ . That is, at equilibrium, the UAVs do not need to provide any horizontal input, but only a vertical input. This is the main reason for, later on, including an integrator along the vertical direction, but not along the horizontal directions.

Let us now parametrize the equilibria with

$$\gamma \in \Gamma := \{(p_\gamma, n_\gamma, F_\gamma) \in \mathbb{R}^3 \times \mathbb{S}^2 \times \mathbb{R}, \quad (14)$$

where  $(p_\gamma, n_\gamma) \in \mathbb{R}^3 \times \mathbb{S}^2$  is the desired pose (linear and angular positions) for the bar; and  $F_\gamma \in \mathbb{R}$  is the desired normal force to be exerted on the bar. The variable  $\gamma$  in (14) is a six-dimensional variable that allows us to parametrize the equilibrium input and the corresponding equilibria. That is, any point in the set  $E := \{(z, u) \in \mathbb{Z} \times \mathbb{R}^6 : Z(z, u) = 0_{24}\}$  can be parametrized by some  $\gamma \in \Gamma$ , i.e.,  $E = \{(z_\gamma, u_\gamma) \in \mathbb{Z} \times \mathbb{R}^6 : \gamma \in \Gamma\}$ , with  $(z_\gamma, u_\gamma)$  as described next (and which can be visualized in Fig. 2). The equilibrium input  $u_\gamma$  is parametrized by  $n_\gamma$  and  $F_\gamma$  as

$$u_\gamma := \begin{bmatrix} u_{1,\gamma} \\ u_{2,\gamma} \end{bmatrix} := \begin{bmatrix} \left(m_1 + \frac{d_2}{d_2 - d_1} m\right) g e_3 + F_\gamma n_\gamma \\ \left(m_2 + \frac{d_1}{d_1 - d_2} m\right) g e_3 - F_\gamma n_\gamma \end{bmatrix}, \quad (16)$$

while the equilibrium state  $z_\gamma := (z_{p,\gamma}, z_{v,\gamma}) := (z_{p,\gamma}, 0_{12})$  is parametrized as (where, below,  $(j, i) \in \{(1, 2), (2, 1)\}$ )

$$z_{p,\gamma} := (p_\gamma, n_\gamma, p_{1,\gamma}, p_{2,\gamma}) \text{ with} \quad (17a)$$

$$p_{j,\gamma} := p_\gamma + d_j n_\gamma + l_j \frac{d_j m g e_3 \pm (d_j - d_i) F_\gamma n_\gamma}{\|d_j m g e_3 \pm (d_j - d_i) F_\gamma n_\gamma\|}. \quad (17b)$$

Figure 2 illustrates the different possible equilibrium configurations.

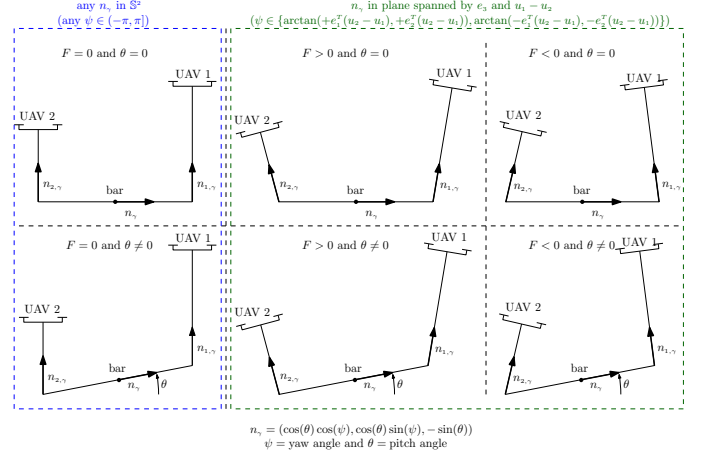


Figure 2: Different equilibrium possibilities, for different values of the pitch angle of the bar –  $\theta \in (-\frac{\pi}{2}, \frac{\pi}{2})$  – and different values of the normal force/stress exerted on the bar –  $F \in \mathbb{R}$ . When  $F > 0$ , the bar is under tension; when  $F < 0$ , the bar is under compression; and, when  $F = 0$ , the bar is under no normal force.

**Remark 5.** Like a pendulum-on-a-cart system, the UAVs-bar system also has infinite open-loop equilibria, with no restrictions on the linear position of the bar. See [36] for a detailed comparison.

### 3.2. Control objective: Pose stabilization of bar

Before introducing the UAVs' attitude dynamics, let us describe the control objective pursued in this paper. The control goal is to design a control law that guarantees pose stabilization of the bar around a desired linear position  $p_\gamma$  and around a desired angular position  $n_\gamma$ , and such that the bar is under a desired normal force  $F_\gamma$ .

**Problem 1.** Let  $\gamma \in \Gamma$ , as in (14), be some chosen desired configuration. Consider then the vector field  $Z$  in (7b), the equilibrium state  $z_\gamma$  in (17), and the equilibrium input  $u_\gamma$  in (16). Design a control law  $u_\gamma^{cl} : \mathbb{Z} \rightarrow \mathbb{R}^6$  satisfying  $u_\gamma^{cl}(z_\gamma) = u_\gamma$  and such that  $z_\gamma$  is a (locally) exponentially stable equilibrium point of the closed-loop vector field  $\mathbb{Z} \ni z \mapsto Z(z, u_\gamma^{cl}(z)) \in T_z \mathbb{Z}$ .

**Remark 6.** The open-loop vector field in (7b) is invariant to translations and rotations around the gravity (which is aligned with the third inertial axis). More precisely, given some rotation  $R \in \{R \in \mathbb{SO}(3) : R e_3 = e_3\}$  and some offset  $o \in \mathbb{R}^3$ , and given

$$z_b = T_{(R,o)}(z_a) := (R(p_a - o), R n_a, R(p_{1,a} - o), R(p_{2,a} - o), R v_a, R w_a, R v_{1,a}, R v_{2,a}) \in \mathbb{Z}, \quad (18a)$$

$$u_b = (R u_{1,a}, R u_{2,a}) \in \mathbb{R}^6, \quad (18b)$$

it follows that

$$\dot{z}_a = Z(z_a, u_a) \Leftrightarrow \dot{z}_b = Z(z_b, u_b). \quad (19)$$

A proof of (19) is found in [36].

### 3.3. Attitude inner-loop

In the previous subsection, the UAVs were assumed fully actuated, that is, each UAV could provide any desired

three dimensional force. This assumption was taken so as to simplify the exposition of the modeling, and, in this section, we explain how we model the fact that the UAVs are not fully actuated. In brief, each UAV has a thrust body direction ( $r_1$  and  $r_2$  in Fig. 1a) along which thrust can be provided; and, we assume we have control over the thrust and the angular velocity of each UAV. For that purpose, recall the state, the constraints, and the state space previously defined in (2), (4) and (5), respectively. Define now the extended state, constraints, and state space

$$\bar{z} \in \mathbb{R}^{30} \Leftrightarrow (z, r_1, r_2) \in \mathbb{R}^{24} \times \mathbb{R}^3 \times \mathbb{R}^3, \quad (20a)$$

$$\bar{f}(\bar{z}) := \begin{bmatrix} f(z) \\ f_7(r_1) \\ f_8(r_2) \end{bmatrix} := \begin{bmatrix} f(z) \\ r_1^T r_1 - 1 \\ r_2^T r_2 - 1 \end{bmatrix}, \quad (20b)$$

$$\bar{Z} := \{\bar{z} \in \mathbb{R}^{30} : \bar{f}(\bar{z}) = 0_s\} = \mathbb{Z} \times \mathbb{S}^2 \times \mathbb{S}^2. \quad (20c)$$

For convenience, denote  $\mathbb{R}_0^6 := \mathbb{R}^6 \setminus \{(0_3, \cdot), (\cdot, 0_3)\}$ . Given an appropriate input  $u : \mathbb{R}_{\geq 0} \rightarrow \mathbb{R}_0^6$ , a system's trajectory  $\bar{z} : \mathbb{R}_{\geq 0} \ni t \mapsto \bar{z}(t) \in \bar{Z}$  evolves according to

$$\dot{\bar{z}}(t) = \bar{Z}(\bar{z}(t), u(t)), \bar{z}(0) \in \bar{Z}, \quad (21a)$$

where the vector field  $\bar{Z} : \bar{Z} \times \mathbb{R}_0^6 \ni (\bar{z}, u) \mapsto \bar{Z}(\bar{z}, u) \in T_{\bar{z}}\bar{Z}$  is given by (recall that  $u = (u_1, u_2)$ )

$$\begin{aligned} \dot{\bar{z}} &= \bar{Z}(\bar{z}, u) \Leftrightarrow \\ \Leftrightarrow \begin{bmatrix} \dot{z} \\ \dot{r}_1 \\ \dot{r}_2 \end{bmatrix} &= \begin{bmatrix} Z\left(z, \begin{bmatrix} U_1 r_1 \\ U_2 r_2 \end{bmatrix}\right) \\ \mathcal{S}(\omega_1) r_1 \\ \mathcal{S}(\omega_2) r_2 \end{bmatrix} := \begin{bmatrix} Z\left(z, \begin{bmatrix} u_1^T r_1 r_1 \\ u_2^T r_2 r_2 \end{bmatrix}\right) \\ \mathcal{S}\left(k_{r,1} \mathcal{S}(r_1) \frac{u_1}{\|u_1\|}\right) r_1 \\ \mathcal{S}\left(k_{r,2} \mathcal{S}(r_2) \frac{u_2}{\|u_2\|}\right) r_2 \end{bmatrix}, \end{aligned} \quad (21b)$$

where  $Z$  is the vector field defined in (7b). Let us give some insight into the vector field in (21b), and let  $i \in \{1, 2\}$ . UAV  $i$  provides a thrust  $U_i$  along its thrust body direction  $r_i$ : moreover,  $U_i = u_i^T r_i$ , and therefore  $U_i r_i = u_i - \Pi(r_i) u_i$  (see definition of  $\Pi$  in Section 2). That means UAV  $i$  provides the desired input  $u_i$ , apart from an error  $\Pi(r_i) u_i$ , which vanishes when the UAV's thrust direction  $r_i$  is aligned with the direction of the input  $u_i$ . On the other hand, UAV  $i$  has an angular velocity  $\omega_i = k_{r,i} \mathcal{S}(r_i) \frac{u_i}{\|u_i\|}$ , where  $k_{r,i} > 0$  is the gain of its attitude inner-loop. This angular velocity steers the UAV's thrust direction  $r_i$  towards the direction of the input  $u_i$ . To gain some intuition, let  $u_i \in \mathbb{R}^3 \setminus \{0_3\}$  be some constant vector and define  $r_i^* = \frac{u_i}{\|u_i\|} \in \mathbb{S}^2$ . Then, if  $\dot{r}_i = \mathcal{S}(k_{r,i} \mathcal{S}(r_i) r_i^*) r_i$ , it follows that, for  $V(r_i) = 1 - r_i^T r_i^* \in [0, 2]$ ,  $\dot{V}(r_i) = DV(r_i) \dot{r}_i = -k_{r,i} \|\mathcal{S}(r_i) r_i^*\|^2 = -V(r_i)(2 - V(r_i)) \leq 0$ , which implies that  $\lim_{t \rightarrow \infty} r_i(t) = r_i^*$  provided that  $r_i(0) \neq -r_i^*$ . The attitude inner-loop gain  $k_{r,i} > 0$  influences how fast the UAV's thrust body direction  $r_i$  is steered towards the direction of the input  $u_i$ .

Given an input satisfying  $\delta_1 = 0_3 \Leftrightarrow u_1 + u_2 = (m_1 + m_2 + m)ge_3$ , it is straightforward to verify that the open-loop equilibria for the vector field in (21b) is given by

$$\bar{E}_u = \{\bar{z} \in \bar{Z} : z \in E_u \text{ and } r_i = \pm u_i / \|u_i\|\}, \quad (22)$$

where the set  $E_u$  is that described in Proposition 4. The equilibria where  $r_i = -u_i / \|u_i\|$  for any or both  $i \in \{1, 2\}$

are unstable, and therefore not considered in the rest of this paper. We can now formulate the problem treated in this paper, as an extension of Problem 1.

**Problem 2.** Let  $\gamma \in \Gamma$  be some chosen desired configuration. Consider then the vector field  $\bar{Z}$  in (21b), the equilibrium state  $z_\gamma$  in (17), and the equilibrium input  $u_\gamma$  in (16). Design a control law  $u_\gamma^{cl} : \mathbb{Z} \rightarrow \mathbb{R}_0^6$  satisfying  $u_\gamma^{cl}(z_\gamma) = u_\gamma$  and such that

$$\bar{z}_\gamma := (z_\gamma, r_{1,\gamma}, r_{2,\gamma}) := (z_\gamma, u_{1,\gamma} / \|u_{1,\gamma}\|, u_{2,\gamma} / \|u_{2,\gamma}\|) \quad (23)$$

is a (locally) exponentially stable equilibrium point of the closed loop vector field  $\bar{Z} \ni \bar{z} \mapsto \bar{Z}(\bar{z}, u_\gamma^{cl}(z)) \in T_{\bar{z}}\bar{Z}$ .

**Remark 7.** A similar remark to that in Remark 6 can be made at this point, that is, (below,  $T$  is as defined in (18))

$$\dot{z}_a = \bar{Z}(z_a, u_a) \Leftrightarrow \dot{z}_b = \bar{Z}(z_b, u_b), \text{ where} \quad (24a)$$

$$\bar{z}_b = \bar{T}_{(R,o)}(\bar{z}_a) := (T_{(R,o)}(z_a), Rr_{1,a}, Rr_{2,a}) \in \bar{Z}, \quad (24b)$$

which implies that the open-loop vector field  $\bar{z} \mapsto \bar{Z}(\bar{z}, u)$  does not see the rotation and offset  $(R, o)$  (for any  $o \in \mathbb{R}^3$  and any  $R \in \{\bar{R} \in \mathbb{SO}(3) : R e_3 = e_3\}$ ).

## 4. Control Law

Let us break down the control law exposition in three subsections. In the first, we introduce a PD-like control law. In the second, we introduce and motivate the need for an integral action term along the vertical direction and for each UAV. In the third, we introduce a saturated version of the former control law, where the saturation guarantees that the control law is bounded and that the desired UAV attitude is well-defined.

### 4.1. PD control law

Recall the problem statement in Problem 2, where a desired pose and normal force are chosen, encapsulated in  $\gamma = (p_\gamma, n_\gamma, F_\gamma)$ . For convenience, denote (hereafter, we assume that  $n_\gamma \neq \pm e_3$ , that is, that we do not require the bar to stand vertically)

$$R_{n_\gamma} \equiv \begin{bmatrix} \frac{\Pi(e_3)n_\gamma}{\sqrt{1-(e_3^T n_\gamma)^2}} & \frac{\mathcal{S}(e_3)n_\gamma}{\sqrt{1-(e_3^T n_\gamma)^2}} & e_3 \end{bmatrix} \in \mathbb{SO}(3), \quad (25a)$$

$$\gamma_\star \equiv (p_\star, n_\star, F_\star)|_{p_\star=0_3, n_\star=(|\cos(\theta_\star)|, 0, -\sin(\theta_\star))}, \quad (25b)$$

where  $\theta_\star, F_\star \in \mathbb{R}$ . We emphasize that the following holds:

$$R_{n_\gamma}^T e_3 = e_3, \quad (25c)$$

$$R_{n_\gamma}^T n_\gamma = \left(\sqrt{1-(e_3^T n_\gamma)^2}, 0, e_3^T n_\gamma\right) = n_{\gamma_\star} \text{ for some } \theta_\star, \quad (25d)$$

$$R_{n_\gamma}^T u_{j,\gamma} \stackrel{(16), (25c), (25d)}{=} u_{j,\gamma_\star} \text{ for } j \in \{1, 2\}. \quad (25e)$$

The necessity of  $R_{n_\gamma}, \gamma_\star$  in (25a), (25b) will be clear next. In brief, the idea is that it will suffice to study  $\gamma_\star$  in (25b) (characterized by the two parameters  $\theta_\star$  and  $F_\star$ ) instead of the  $\gamma$  in (14) (characterized by six parameters).

Given a  $\gamma$ , consider then the control law  $u_\gamma^{pd}$ , combining a feed-forward (FF) term with a PD term, given by

$$z \mapsto u_\gamma^{pd}(z) := \underbrace{\begin{bmatrix} u_{1,\gamma}^{pd}(z) \\ u_{2,\gamma}^{pd}(z) \end{bmatrix}}_{\text{FF in (16)}} + \underbrace{\begin{bmatrix} \tilde{u}_{1,\gamma}^{pd}(z) \\ \tilde{u}_{2,\gamma}^{pd}(z) \end{bmatrix}}_{\text{PD term}}, \quad (26)$$



where, for each UAV  $j \in \{1, 2\}$ ,

$$\tilde{u}_{j,\gamma}^{pd}(z) := -m_j R_{n_\gamma} \left( K_p^j R_{n_\gamma}^T (p_j - p_{j,\gamma}) + K_d^j R_{n_\gamma}^T v_j \right) - m_j d_j e_3^T (k_{p,\psi}^j \mathcal{S}(n_\gamma) n + k_{d,\psi}^j \omega) R_{n_\gamma} e_2, \quad (27)$$

and where: (i)  $p_{1,\gamma}, p_{2,\gamma} \in \mathbb{R}^3$  are the UAVs' desired equilibrium positions given in (17b); (ii)  $K_p^j = k_{p,x}^j \oplus k_{p,y}^j \oplus k_{p,z}^j \in \mathbb{R}^{3 \times 3}$  and  $K_d^j = k_{d,x}^j \oplus k_{d,y}^j \oplus k_{d,z}^j \in \mathbb{R}^{3 \times 3}$  are positive gains related to the position and velocity feedback, respectively, of vehicle  $j \in \{1, 2\}$ ; (iii)  $k_{p,\psi}^j \in \mathbb{R}_{\geq 0}$  and  $k_{d,\psi}^j \in \mathbb{R}_{\geq 0}$  are gains related to the angular position and angular velocity feedback.

Note that  $\tilde{u}_{\gamma}^{pd}(z_\gamma) = 0_6$ , and therefore  $u_{\gamma}^{pd}(z_\gamma) = u_\gamma$ , as required in Problem 2. Let us provide some insight into the control law in (26), and recall that we wish to steer the linear position of the bar  $p$  to  $p_\gamma$  and to steer the angular position of the bar  $n$  to  $n_\gamma$ . Finally, and for brevity, let us introduce the following nomenclature (where we make use of  $R_{n_\gamma}$  defined in (25a)):  $R_{n_\gamma} e_1$  corresponds to the longitudinal direction, or  $x$ -direction (when seen from above, this direction is aligned with the desired angular position of the bar  $n_\gamma$ );  $R_{n_\gamma} e_2$  corresponds to the lateral direction, or  $y$ -direction; and  $R_{n_\gamma} e_3 = e_3$  corresponds to the vertical direction, or  $z$ -direction. For example, when  $n_\gamma = e_1$  (or when  $n_\gamma = (\cos(\theta), 0, -\sin(\theta))$ ), then  $R_{n_\gamma} = I_3$ : i.e., when the desired angular position is aligned with the first inertial axis, then the longitudinal direction corresponds to the first inertial axis, and the lateral direction corresponds to the second inertial axis.

The control law in (27) may be decomposed in two identifiable parts. (i) Along each component – longitudinal, lateral and vertical – there are two terms, one proportional and one derivative, that act as a spring-damper that brings the UAV to its desired longitudinal/lateral/vertical position. (ii) In addition, along the lateral component, there are two more terms (one proportional and one derivative) that assist in bringing the bar to its desired angular position.

**Remark 8.** Recall Remark 6, where we established that the open-loop vector field does not see translations and rotations around the gravity. Recall also (25). It is easy to verify that, for  $j \in \{1, 2\}$ , ( $T$  as defined in (18))

$$u_{j,\gamma}^{pd}(z) = R_{n_\gamma} u_{j,\gamma_\star}^{pd} \left( T_{(R_{n_\gamma}^T, p_\gamma)}(z) \right), \quad (28)$$

for any  $z \in \mathbb{Z}$  and any  $\gamma \in \Gamma$ ; which combined with Remark 6 implies that the closed-loop vector field  $z \mapsto Z(z, u_{\gamma}^{pd}(z))$  does not see the rotation and offset ( $R_{n_\gamma}^T, p_\gamma$ ). That means we can study only the closed-loop vector field  $z \mapsto Z(z, u_{\gamma_\star}^{pd}(z))$ , where we want to stabilize the bar around the origin, and aligned with the positive first-axis – see (25b). As such, when studying the different equilibrium possibilities encapsulated in  $\gamma$ , there are only two parameters that are worth studying, namely the desired pitch angle of the bar  $\theta_\star$  and the desired normal force to be exerted on the bar  $F_\star$ .

The control law in (26) has three flaws. (i) The terms  $u_{1,\gamma}, u_{2,\gamma}$  are model dependent, and therefore sensitive to

modeling identification errors (such as an unknown bar mass) – addressed in Subsection 4.2. (ii) The control law is unbounded: that is,  $\|u_{j,\gamma}^{pd}(z)\|$  is arbitrarily large when the UAV's linear position  $p_j$  is arbitrarily far away from its desired linear position  $p_{j,\gamma}$  – addressed in Subsection 4.3. (iii) When the bar's angular position  $n$  is (close to) diametrically opposed to its desired angular position  $n_\gamma$ , the control law encourages the UAVs to swap positions rather than encouraging the bar to rotate around the vertical direction, and this issue is addressed in [36].

#### 4.2. Integral action and PID control law

The control law in (26) is heavily dependent on the exact knowledge of model parameters. Suppose, for simplicity, that we wish the bar to be under no normal force, that is,  $F_\gamma = 0$ . Then, it follows from (16) that  $u_{1,\gamma} = \left( m_1 g + \frac{d_2}{d_2 - d_1} m g \right) e_3$ , that is, UAV 1 needs to have an exact knowledge of its weight, of the bar's weight, and of the contact points on the bar (an interchangeable conclusion may be drawn for UAV 2). Note, however, that only the third (vertical) component of  $u_{1,\gamma}$  is model dependent, while the first and second (horizontal) components are zero and, therefore, model independent. This is the motivation for including an integral action in the vertical component of the control laws of each UAV (and to suppress such integral action in the horizontal components).

For that purpose, and with (20) in mind, define now the extended state, constraints, and state space

$$\tilde{z} \in \mathbb{R}^{32} : \Leftrightarrow (\tilde{z}, \xi_{1,z}, \xi_{2,z}) \in \mathbb{R}^{30} \times \mathbb{R} \times \mathbb{R}, \quad (29a)$$

$$\tilde{f}(\tilde{z}) := \tilde{f}(\tilde{z}), \quad (29b)$$

$$\tilde{\mathbb{Z}} := \{ \tilde{z} \in \mathbb{R}^{32} : \tilde{f}(\tilde{z}) = 0_8 \} = \tilde{\mathbb{Z}} \times \mathbb{R} \times \mathbb{R}, \quad (29c)$$

where  $\xi_{1,z}, \xi_{2,z}$  are the integral action terms for UAVs 1, 2.

Given an appropriate input  $u : \mathbb{R}_{\geq 0} \rightarrow \mathbb{R}_0^6$ , a system's trajectory  $\tilde{z} : \mathbb{R}_{\geq 0} \ni t \mapsto \tilde{z}(t) \in \tilde{\mathbb{Z}}$  evolves according to

$$\dot{\tilde{z}}(t) = \tilde{Z}_\gamma(\tilde{z}(t), u(t)), \tilde{z}(0) \in \tilde{\mathbb{Z}}, \quad (30a)$$

where the vector field  $\tilde{Z}_\gamma : \tilde{\mathbb{Z}} \times \mathbb{R}_0^6 \ni (\tilde{z}, u) \mapsto \tilde{Z}_\gamma(\tilde{z}, u) \in T_{\tilde{z}} \tilde{\mathbb{Z}}$  is given by

$$\dot{\tilde{z}} = \tilde{Z}_\gamma(\tilde{z}, u) : \Leftrightarrow \begin{bmatrix} \dot{\tilde{z}} \\ \dot{\xi}_{1,z} \\ \dot{\xi}_{2,z} \end{bmatrix} = \begin{bmatrix} \bar{Z}(\tilde{z}, u) \\ e_3^T(p_1 - p_{1,\gamma}) \\ e_3^T(p_2 - p_{2,\gamma}) \end{bmatrix}, \quad (30b)$$

where  $\bar{Z}$  is the vector field defined in (21b). The integral action equations in (30b) enforce that an equilibrium can only be reached if the UAVs are at the desired height, i.e., if  $e_3^T(p_i - p_{i,\gamma}) = 0$ . Note also that the open-loop vector field in (30b) depends on  $\gamma$ , and thus the reason for indexing  $\gamma$  in  $\tilde{Z}_\gamma$ .

**Remark 9.** Recall Remark 7. It is easy to verify that (below,  $\bar{T}$  is as defined in (24b))

$$\dot{\tilde{z}}_a = \tilde{Z}_\gamma(\tilde{z}_a, u_a) \Leftrightarrow \dot{\tilde{z}}_b = \tilde{Z}_\gamma(\tilde{z}_b, u_b), \text{ where} \quad (31)$$

$$\tilde{z}_b = \bar{T}_{(R,o)}(\tilde{z}_a) := (\bar{T}_{(R,o)}(\tilde{z}_a), \xi_{1,z,a}, \xi_{2,z,a}), \quad (32)$$

which implies that the open-loop vector field  $\tilde{z} \mapsto \tilde{Z}_\gamma(\tilde{z}, u)$  does not see the rotation and offset  $(R, o)$  (for any  $o \in \mathbb{R}^3$

and any  $R \in \{R \in \mathbb{SO}(3) : Re_3 = e_3\}$ .

Denote  $\hat{u}_{1,\gamma}$  and  $\hat{u}_{2,\gamma}$  as the best estimates of  $u_{1,\gamma}$  and  $u_{2,\gamma}$  known by UAVs 1 and 2, respectively<sup>3</sup>. With the control law (26) in mind, consider then the PID-like control law

$$\tilde{z} \mapsto u_\gamma^{pid}(\tilde{z}) := \begin{bmatrix} \hat{u}_{1,\gamma} \\ \hat{u}_{2,\gamma} \end{bmatrix} + \begin{bmatrix} \tilde{u}_{1,\gamma}^{pd}(z) \\ \tilde{u}_{2,\gamma}^{pd}(z) \end{bmatrix} + \begin{bmatrix} m_1 k_{i,z}^1 \xi_{1,z} e_3 \\ m_2 k_{i,z}^2 \xi_{2,z} e_3 \end{bmatrix} \quad (33)$$

where  $\xi_{j,z}$  is the integral action term for UAV  $j$ ; where  $k_{i,z}^j$  is the respective integral gain; and where  $\tilde{u}_{j,\gamma}^{pd}$  is the PD control law in (27). It follows immediately that, for

$$\tilde{z}_\gamma := \begin{bmatrix} \tilde{z}_\gamma \\ \xi_{1,z,\gamma} \\ \xi_{2,z,\gamma} \end{bmatrix} := \begin{bmatrix} \tilde{z}_\gamma \\ \frac{1}{m_1 k_{i,z}^1} e_3^T (u_{1,\gamma} - \hat{u}_{1,\gamma}) \\ \frac{1}{m_2 k_{i,z}^2} e_3^T (u_{2,\gamma} - \hat{u}_{2,\gamma}) \end{bmatrix}, \quad (34)$$

it holds that  $u_\gamma^{pid}(\tilde{z}_\gamma) = u_\gamma$ , and therefore  $\tilde{z}_\gamma$  is an equilibrium point of the closed loop vector field

$$\tilde{Z} \ni \tilde{z} \mapsto \tilde{Z}_\gamma(\tilde{z}, u_\gamma^{pid}(\tilde{z})) \in T_{\tilde{z}} \tilde{Z}. \quad (35)$$

Note that it is the purpose of the integral action terms to make sure that the equality  $u_\gamma^{pid}(\tilde{z}_\gamma) = u_\gamma$  is satisfied. Loosely speaking, the integral action terms  $\xi_{1,z}$ ,  $\xi_{2,z}$  evolve so as to compensate for the model mismatch; in particular, if all model parameters are exactly known by both UAVs, then  $\xi_{1,z,\gamma} = \xi_{2,z,\gamma} = 0$  (even if all model parameters are exactly known, it is still a good practical solution to include integral action terms, as they provide robustness against other types of uncertainty). Finally, note that the control law  $u_\gamma^{pid}$  in (33) only differs from  $u_\gamma^{pd}$  in (26) along the vertical direction, and therefore the integral action terms are expected to influence only the vertical linear and vertical angular motions of the bar (and this is indeed the case when  $\theta_* = 0$  and  $F_* = 0$ ).

**Remark 10.** Recall Remark 9, where we established that the open-loop vector field does not see the rotation and offset  $(R, o)$ . Recall also (25). It is easy to verify that, for  $j \in \{1, 2\}$ , (below,  $\tilde{T}$  as defined in (32))<sup>4</sup>

$$u_{j,\gamma}^{pid}(\tilde{z}) = R_{n_\gamma} u_{j,\gamma}^{pid} \left( \tilde{T}_{(R_{n_\gamma}^T, p_\gamma)}(\tilde{z}) \right), \quad (36)$$

which combined with Remark 9 implies that the closed-loop vector field  $\tilde{z} \mapsto \tilde{Z}_\gamma(\tilde{z}, u_\gamma^{pid}(\tilde{z}))$  does not see the rotation and offset  $(R_{n_\gamma}^T, p_\gamma)$ . That means we can study only the closed-loop vector field  $\tilde{z} \mapsto \tilde{Z}_{\gamma_*}(\tilde{z}, u_\gamma^{pid}(z))$ , where the want to stabilize the bar around the origin, and aligned with the positive first-axis – see (25b). As such, when studying the different equilibrium possibilities encapsulated in  $\gamma$ , there are only two parameters that are worth studying, namely the desired pitch angle of the bar  $\theta_*$  and the desired normal force to be exerted on the bar  $F_*$ .

<sup>3</sup>We emphasize that the term  $\pm F_\gamma n_\gamma$  in (16) is model independent, but, as discussed in Section 3.1, it requires synchrony between the UAVs. Moreover, the estimate  $\hat{u}_{j,\gamma}$  only differs from the real  $u_{j,\gamma}$  along the vertical direction, i.e.,  $\Pi(e_3)(\hat{u}_{j,\gamma} - u_{j,\gamma}) = 0_3$ .

<sup>4</sup>Since  $\Pi(e_3)(\hat{u}_{j,\gamma} - u_{j,\gamma}) = 0_3 \Leftrightarrow \hat{u}_{j,\gamma} = u_{j,\gamma} + k e_3$  for some  $k \in \mathbb{R}$ , it follows immediately from (25c)–(25e) that  $R_{n_\gamma}^T \hat{u}_{j,\gamma} = \hat{u}_{j,\gamma_*}$ . This is necessary when proving (36).

#### 4.3. Bounded control law

From a practical perspective, it is important to guarantee that the control laws for each UAV are bounded, since each UAV has actuation limitations. On the other hand, from a well-posedness perspective, it is important to guarantee that the control laws for each UAV do not vanish. Indeed, recall from Section 3.3, that the desired attitude for UAV  $i$  is given by  $\frac{u_i}{\|u_i\|}$ , which is only well defined provided that  $u_i$  does not vanish (which one is able to guarantee by appropriately saturating the proportional, derivative and integral terms).

Let  $\sigma$  be some positive constant and  $\text{sat}_\sigma : \mathbb{R} \rightarrow [-\sigma, +\sigma]$  be some saturation function, satisfying  $\text{sat}_\sigma(0) = 0$ ,  $0 < \text{sat}'_\sigma(\cdot) \leq 1$ ,  $\text{sat}'_\sigma(0) = 1$  (for example,  $x \mapsto \text{sat}_\sigma(x) := \frac{\sigma x}{\sqrt{\sigma^2 + x^2}}$  is a possible saturation function).

With the control law  $u_\gamma^{pid}$  in (33) in mind, the real control law is then given by that in (37), for UAV  $j \in \{1, 2\}$ , for some positive  $\sigma_{p,x}^j, \sigma_{d,x}^j, \sigma_{p,y}^j, \sigma_{d,y}^j, \sigma_{p,z}^j, \sigma_{d,z}^j, \sigma_{i,z}^j, \sigma_{d,\psi}^j$  (for example,  $\sigma_{p,x}^j$  corresponds to a saturation on the longitudinal position error of UAV  $j$ ).

Consider  $\bar{u}_j$  as defined in (38), and let the gains and saturations be chosen such that  $\bar{u}_j < \|\hat{u}_{j,\gamma}\|$ . Then, it can be verified that

$$0 < \|\hat{u}_{j,\gamma}\| - \bar{u}_j \leq \|u_\gamma^{pid}(\cdot)\| \leq \|\hat{u}_{j,\gamma}\| + \bar{u}_j \quad (39)$$

and, as such, the control input required from each UAV is bounded, and, simultaneously, the desired attitude for each UAV, given by  $\frac{u_\gamma^{pid}(\cdot)}{\|u_\gamma^{pid}(\cdot)\|}$ , is also well defined.

If, in addition, the integral saturations are chosen big enough, specifically if  $\sigma_{i,z}^j > \left| \frac{e_3^T (u_{j,\gamma} - \hat{u}_{j,\gamma})}{m_j} \right|$  for  $j \in \{1, 2\}$ , then it follows that  $u_\gamma^{pid}(\tilde{z}_\gamma) = u_\gamma \Rightarrow \tilde{Z}_\gamma(\tilde{z}_\gamma, u_\gamma^{pid}(\tilde{z}_\gamma)) = 0_{32}$  for

$$\tilde{z}_\gamma := \begin{bmatrix} \tilde{z}_\gamma \\ \xi_{1,z,\gamma} \\ \xi_{2,z,\gamma} \end{bmatrix} := \begin{bmatrix} \tilde{z}_\gamma \\ \frac{1}{k_{i,z}^1} (\text{sat}_{\sigma_{i,z}^1})^{-1} \left( \frac{e_3^T (u_{1,\gamma} - \hat{u}_{1,\gamma})}{m_1} \right) \\ \frac{1}{k_{i,z}^2} (\text{sat}_{\sigma_{i,z}^2})^{-1} \left( \frac{e_3^T (u_{2,\gamma} - \hat{u}_{2,\gamma})}{m_2} \right) \end{bmatrix}, \quad (40)$$

that is,  $\tilde{z}_\gamma$  above is an equilibrium point under the saturated control law (and it degenerates into (34) when  $\text{sat}_{\sigma_{i,z}^1}$  and  $\text{sat}_{\sigma_{i,z}^2}$  are the identity functions).

**Remark 11.** Later in this paper, we perform a linearization of the (closed-loop) vector field

$$\tilde{z} \mapsto \tilde{Z}^{cl}(\tilde{z}) := \tilde{Z}_\gamma(\tilde{z}, u_\gamma^{pid}(\tilde{z})) \quad (41)$$

around the equilibrium point  $\tilde{z}_\gamma$  (with  $\tilde{Z}_\gamma$ ,  $u_\gamma^{pid}$ ,  $\tilde{z}_\gamma$  defined in (30b), (37), (40)). Let us then discuss the impact the saturations (in the control law in (37)) have on the linearization. For that purpose, recall the vector field  $\tilde{Z}$  in (21b) and recall that  $Z$  in (7b) is input affine (see Remark 2). For that reason, the  $\dot{z}$  part in (21b) is linear w.r.t.  $(u_1, u_2)$ , while the  $\dot{r}_i$  part in (21b) is linear w.r.t.  $\frac{u_i}{\|u_i\|}$ .

Now, denote  $\text{id} : \mathbb{R} \ni x \mapsto x \in \mathbb{R}$  as the identity function, and recall that the control law with saturations (in (37)) degenerates into the control law without saturations (in (33)) when  $\text{sat}_\sigma = \text{id}$ . It may then be verified that



$$u_{j,\gamma}^{pid}(\tilde{z}) = \hat{u}_{j,\gamma} - m_j R_{n_\gamma} \begin{bmatrix} k_{p,x}^{j,\gamma} \text{sat}_{\sigma_{p,x}^j}((R_{n_\gamma} e_1)^T(p_j - p_{j,\gamma})) + k_{d,x}^{j,\gamma} \text{sat}_{\sigma_{d,x}^j}((R_{n_\gamma} e_1^T)v_j) \\ k_{p,y}^{j,\gamma} \text{sat}_{\sigma_{p,y}^j}((R_{n_\gamma} e_2)^T(p_j - p_{j,\gamma})) + k_{d,y}^{j,\gamma} \text{sat}_{\sigma_{d,y}^j}((R_{n_\gamma} e_2^T)v_j) \\ k_{p,z}^{j,\gamma} \text{sat}_{\sigma_{p,z}^j}((R_{n_\gamma} e_3)^T(p_j - p_{j,\gamma})) + k_{d,z}^{j,\gamma} \text{sat}_{\sigma_{d,z}^j}((R_{n_\gamma} e_3^T)v_j) \end{bmatrix} - m_j R_{n_\gamma} \begin{bmatrix} 0 \\ d_j (k_{p,\psi}^{j,\gamma} e_3^T S(n_\gamma) n + k_{d,\psi}^{j,\gamma} \text{sat}_{\sigma_{d,\psi}^j}(e_3^T \omega)) \\ \text{sat}_{\sigma_{i,z}^j}(k_{i,z}^{j,\gamma} \xi_{j,z}) \end{bmatrix} \quad (37)$$

$$\bar{u}_j := m_j \sqrt{\sum_{l \in \{x,y,z\}} (k_{p,l}^{j,\gamma} \sigma_{p,l}^j + k_{d,l}^{j,\gamma} \sigma_{d,l}^j)^2 + d_j (k_{p,\psi}^{j,\gamma} + k_{d,\psi}^{j,\gamma} \sigma_{d,\psi}^j)^2 + (\sigma_{i,z}^j)^2} \quad (38)$$

(for brevity, denote  $\alpha_j = \text{sat}'\left(\text{sat}^{-1}\left(\frac{\hat{u}_{j,\gamma} - u_{j,\gamma}}{m_j}\right)\right)$  where  $\text{sat} \equiv \text{sat}_{\sigma_{i,z}^j}$ ; and let  $\xrightarrow{r,b}$  read as  $\xrightarrow{\text{replaced by}}$ )

$$\frac{\partial}{\partial \tilde{z}} u_{j,\gamma}^{pid}(\tilde{z})|_{\tilde{z}=\tilde{z}_\gamma} = \left( \frac{\partial}{\partial \tilde{z}} u_{j,\gamma}^{pid}(\tilde{z}_\gamma)|_{\tilde{z}=\tilde{z}_\gamma} \right) \Big|_{\substack{\text{sat}_{\sigma_{i,z}^j}^{r,b} id \\ k_{i,z}^{j,\gamma} \xrightarrow{r,b} \alpha_j k_{i,z}^{j,\gamma}}} \quad (42a)$$

which in turn implies that

$$\frac{\partial}{\partial \tilde{z}} \frac{u_{j,\gamma}^{pid}(\tilde{z})}{\|u_{j,\gamma}^{pid}(\tilde{z})\|} \Big|_{\tilde{z}=\tilde{z}_\gamma} = \left( \frac{\partial}{\partial \tilde{z}} \frac{u_{j,\gamma}^{pid}(\tilde{z})}{\|u_{j,\gamma}^{pid}(\tilde{z})\|} \Big|_{\tilde{z}=\tilde{z}_\gamma} \right) \Big|_{\substack{\text{sat}_{\sigma_{i,z}^j}^{r,b} id \\ k_{i,z}^{j,\gamma} \xrightarrow{r,b} \alpha_j k_{i,z}^{j,\gamma}}} \quad (42b)$$

It follows from (42a)–(42b) that the linearization is insensitive to the saturations, provided that the integral gains of the unsaturated control law in (33) are replaced as  $k_{i,z}^{j,\gamma} \xrightarrow{r,b} \alpha_j k_{i,z}^{j,\gamma}$ , for  $j \in \{1, 2\}$  (in particular, when  $\hat{u}_{j,\gamma} = u_{j,\gamma}$ , then  $\alpha_j = \text{sat}'(\text{sat}^{-1}(0)) = 1$ , which corresponds to no replacement).

**Remark 12.** Recall Remark 10, where we established that the closed-loop vector field  $\tilde{z} \mapsto \tilde{Z}_\gamma(\tilde{z}, u_\gamma^{pid}(\tilde{z}))$  does not see the rotation and offset  $(R_{n_\gamma}^T, p_\gamma)$  for the PID control law without saturations in (33). For the PID-control law with saturations in (37) that conclusion no longer holds (the control law is not insensitive to arbitrary translations, owing to the presence of the saturations). However, the results presented later in this paper are of a local nature, and, as we have established in Remark 11, at the equilibrium, the saturated control law in (37) behaves exactly the same way as the unsaturated control law in (33) provided that the integral gains are appropriately scaled.

## 5. Conditions for Local Stability

In Section 6, we linearize the closed-loop vector field around the equilibrium, and we verify that the Jacobian is similar to a block triangular matrix, whose block diagonal entries are in controllable form. This section provides immediate tools for the analysis of the eigenvalues of those matrices in controllable form. Denote then, for any  $n \in \mathbb{N}$ ,

$$C_n(a) := [e_2 \quad \dots \quad e_n \quad -a]^T \in \mathbb{R}^{n \times n} \quad (43)$$

as a matrix in controllable form, and whose eigenvalues are those in  $\{\lambda \in \mathbb{C} : \sum_{i=0}^{i=n} a_i \lambda^i = 0\}$  ( $a \in \mathbb{R}^n$  and  $e_i$  is the  $i$ -th canonical basis vector in  $\mathbb{R}^n$ ). It follows from the Routh's criterion that

$$C_3((a_0, a_1, a_2)) \text{ Hurwitz} \Leftrightarrow a_0, a_1, a_2 > 0 \wedge a_0 < a_1 a_2, \quad (44)$$

which we make use of later on. In what follows, denote  $q \in \mathbb{R}$ ,  $f := (f_p, f_d) \in (\mathbb{R}_{\geq 0})^2$ ,  $k := (k_p, k_d) \in (\mathbb{R}_{\geq 0})^2$ , where, in later sections,  $q$  and  $f$  provide physical constants of interest, and  $k$  provides the controller gains (in particular a

proportional and a derivative gain). There are matrices (in controllable form) that appear several times in Section 6, and therefore we introduce them here. Specifically, we define  $\Gamma_3$  and  $\Gamma_5$  as

$$\Gamma_3(f, k) := C_3((f_d(k_p + f_p), f_d k_d + f_p, f_d)), \quad (45a)$$

$$\Gamma_5(q, f, k) := C_5(b_1 + b_2) \Big|_{\substack{b_1 \equiv f_d(f_p k_p, f_p k_d, k_p, k_d, 1) \\ b_2 \equiv f_p(1+q)(0, 0, f_d, 1, 0)}} \quad (45b)$$

Since we are interested in determining the stability of an equilibrium, it proves useful to determine when a matrix is Hurwitz. That is the case iff all the elements in the first column of the Routh's table are positive (or negative) [38] (these columns are found in the mathematica files in [36]). It follows from the Routh's criterion that (45a) and (45b) are Hurwitz if and only if

$$q > 0 \text{ and } f_d > k_p/k_d. \quad (45c)$$

We also define  $\tilde{\Gamma}_4$  and  $\tilde{\Gamma}_4$  as

$$\tilde{\Gamma}_4(\tilde{q}, q, f_p, k) := C_4((f_p(k_p + f_p q \tilde{q}), f_p k_d, k_p + f_p(1+q), k_d)), \quad (46a)$$

$$\Gamma_4(q, f_p, k) := \tilde{\Gamma}_4(0, q, f_p, k), \quad (46a)$$

and it follows from the Routh's criterion that  $\Gamma_4$  is Hurwitz iff  $q > 0$ , and that  $\tilde{\Gamma}_4$  is Hurwitz iff

$$q(1 - \tilde{q}) > 0 \text{ and } k_p > -f_p q \tilde{q}. \quad (46b)$$

## 6. Stability Analysis of the Closed-Loop System

### 6.1. Linearization around a point in a manifold

Before linearizing the closed-loop vector field  $\tilde{Z}_\gamma^{cl}$  in (41) around the equilibrium  $\tilde{z}_\gamma$  in (40), let us provide a vector field that serves only analysis purposes.

For that purpose, consider then the constraints, the state space and the vector field

$$f : \mathbb{R}^n \ni y \mapsto f(y) \in \mathbb{R}^m, \quad (47a)$$

$$\mathbb{Y} := \{y \in \mathbb{R}^n : f(y) = 0_m\}, \quad (47b)$$

$$Y : \mathbb{Y} \ni y \mapsto Y(y) \in T_y \mathbb{Y}, \quad (47c)$$

and suppose that the vector field  $Y$  vanishes at  $y^* \in \mathbb{Y}$ , i.e.,  $Y(y^*) = 0_n$ . The constraints map  $f$  above is assumed smooth, and, since  $Y(y) \in T_y \mathbb{Y}$ , it is the case that  $Df(y)Y(y) = 0_m$  for all  $y \in \mathbb{Y}$ . Finally, we assume that  $Df(y^*) \in \mathbb{R}^{m \times n}$  is full rank.

If one linearizes  $Y$  around  $y^*$ , the resulting Jacobian has  $m$  poles that need to be ignored, as these correspond to eigenvalues in directions the system will never exploit. For that purpose, consider then, for any  $y \in \mathbb{R}^n$  and for some  $\lambda > 0$ , (below, denote  $P_\perp \equiv Df(y^*)$ )

$$Y^*(y) := Y(y) - P_\perp^T (P_\perp P_\perp^T)^{-1} (Df(y)Y(y) + \lambda f(y)) \quad (48)$$

(the inverse above is well defined since  $Df(y^*)$  is full rank) where it follows from (47), that for any  $y \in \mathbb{Y}$ ,  $Y^*(y) =$

$Y(y)$ . As such, the vector field  $Y^*$  and  $Y$  yield the same trajectories provided that a trajectory starts in  $\mathbb{Y}$ , and which proves the following result.

**Proposition 13.** *Let  $Y$  be a vector field in  $\mathbb{Y}$ , as defined in (47), and with  $y^* \in \mathbb{Y}$  as an equilibrium point (e.q.). Then,  $y^*$  is an exponentially stable e.q. of  $Y$  if and only if  $y^*$  is an exponentially stable e.q. of  $Y^*$ , as defined in (48).*

Linearizing  $Y^*$  around  $y^*$  yields the Jacobian  $DY^*(y^*)$ , which is given by

$$DY^*(y^*) = (\Pi_{P_\perp} DY(y^*) - \lambda P_\perp^T (P_\perp P_\perp^T)^{-1} P_\perp), \quad (49)$$

$$\Pi_{P_\perp} := I_n - P_\perp^T (P_\perp P_\perp^T)^{-1} P_\perp \in \mathbb{R}^{n \times n},$$

and where we have used the fact that  $Y(y^*) = 0_n$ , and where the matrix  $\Pi_{P_\perp}$  corresponds to a projection onto the space orthogonal to the directions spanned by  $P_\perp^T = Df(y^*)^T \in \mathbb{R}^{n \times m}$ . Let  $P := [P_1^T \ P_\perp^T]^T$  and  $P^{-1} \equiv [Q_1 \ Q_2]$ , where  $P$  is some change of basis matrix (and therefore invertible). It then follows that the Jacobian  $DY^*(y^*)$  is similar to a block triangular matrix, specifically

$$PDY^*(y^*)P^{-1} = \begin{bmatrix} P_1 \Pi_{P_\perp} DY(y^*) \Pi_{P_\perp} Q_1 & \star_{(n-m) \times m} \\ 0_{m \times (n-m)} & -\lambda I_m \end{bmatrix} \quad (50)$$

The purpose of  $Y^*$  is now clear: the  $m$  poles of the Jacobian  $DY(y^*)$  associated to the directions spanned by  $P_\perp = Df(y^*)^T$  have been replaced by  $m$  poles at  $-\lambda < 0$ . As such, in order to determine the stability properties of the equilibrium  $y^*$ , it suffices to study whether the upper-left matrix in (50) is Hurwitz. A proof of the derivation of (50) is found in [36].

**Remark 14.** *It can now be seen from (48) why we needed to provide the constraints' maps  $f$ ,  $\tilde{f}$  and  $\hat{f}$  defined in (4), (20) and (29).*

## 6.2. Linearization of the closed-loop vector field

Recall now the closed-loop vector field  $\tilde{Z}_\gamma^{cl}$  in (41) and the equilibrium point  $\tilde{z}_\gamma$  in (40). Recall also Remark 12, where we concluded that it suffices to study  $\gamma_*$  (instead of  $\gamma$ ). Given that the motion of our system is constrained in a manifold and for the reasons described in the previous subsection, we modify the vector field as in (48) (this change serves only the purpose of analysis). We then compute the Jacobian

$$A := D(\tilde{Z}_{\gamma_*}^{cl})^*(\tilde{z}_{\gamma_*}) \in \mathbb{R}^{32 \times 32} |_{(\tilde{Z}_{\gamma_*}^{cl})^* \text{ as defined in (48)}}, \quad (51)$$

which is sparse, but unstructured (in (51),  $Y \equiv \tilde{Z}_{\gamma_*}^{cl}$ , and  $Y^* \equiv (\tilde{Z}_{\gamma_*}^{cl})^*$ , with  $Y^*$  as defined in (48)). Moreover, the Jacobian is neither a diagonal nor a triangular matrix, and thus determining whether it is Hurwitz is not straightforward. For that purpose, we provide a change of basis matrix

$$P := [P_1 \ \cdots \ P_k \ P_\perp]^T, \quad (52a)$$

for some  $k \in \mathbb{N}$ , such that  $PAP^{-1}$  is a block triangular matrix, i.e.,

$$PAP^{-1} = \begin{bmatrix} A_1 \oplus \cdots \oplus A_k & \star \\ 0 & -\lambda I \end{bmatrix}. \quad (52b)$$

That is, we provide a change of basis that breaks the motion of the system into  $k$  decoupled motions (note that the  $\lambda > 0$  in (52b) is that chosen in (48)). Thus  $\text{eig}(A) = \{-\lambda\} \cup \text{eig}(A_1) \cup \cdots \cup \text{eig}(A_k)$ , and, therefore, determining whether the Jacobian  $A$  in (51) is Hurwitz amounts to checking whether each of the blocks in (52b) is Hurwitz.

Recall Remark 10, where we established that there are only two equilibrium parameters worth studying, namely the desired normal force to be exerted on the bar  $F_*$  and the desired pitch angle of the bar  $\theta_*$ . In the next four subsections, we analyze four separate cases: in Section 6.3, we assume that the system is symmetric and that  $(\theta_*, F_*) = (0, 0)$ ; in Section 6.4, we let the system be asymmetric, while still requiring that  $(\theta_*, F_*) = (0, 0)$ ; in Section 6.5, we let  $\theta_* \neq 0$  and  $F_* = 0$ ; and, finally, in Section 6.6, we let  $\theta_* = 0$  and  $F_* \neq 0$  (for simplicity, in both Sections 6.5 and 6.6 we let the UAVs be fully actuated). Analyzing the most generic of cases (one where the system is asymmetric, the pitch is non-zero, and the normal force is also non-zero) may be done following a similar approach, but it is left for future research.

## 6.3. Symmetric UAVs-bar system

Let us discuss first the case where the UAVs-bar system is symmetric, i.e., when the cables have the same length; when the contacts points on the bar are at the same distance away from the bar's center-of-mass (but in opposite directions); and, when the UAVs are identical, with the same weights and the same control law gains (and where we let  $k_{p,\psi}^j = 0$  and  $k_{d,\psi}^j = 0$  for  $j \in \{1, 2\}$ ). These conditions are summarized in (70). This case provides us with intuition on how to decompose the Jacobian into three decoupled motions (vertical, longitudinal and lateral), and it is the basis for the generic case where the system does not satisfy the symmetry conditions in (70).

Consider then the Jacobian  $A$  in (51), and the change of basis matrix

$$P := [P_z \ P_\theta \ P_x \ P_\delta \ P_y \ P_\psi \ P_\perp]^T \in \mathbb{R}^{32 \times 32}, \quad (53)$$

with its entries listed in Table 1, and where  $P_\perp := (D\tilde{f}(\tilde{z}_\gamma))^T \in \mathbb{R}^{32 \times 8}$  (where  $\tilde{f}$  is the constraints map defined in (29b) – see Section 6.1). It can be calculated that  $|P| = -\frac{d^3 g^{13} m^3 (m+2M)^4}{4J^3 L^{13} M^4}$ , which is non-zero provided that  $d \neq 0$  (when  $d_1 = -d_2 = d = 0$ , the bar's angular velocity is constant and equal to its initial condition, which implies that the bar's angular position is uncontrollable – this agrees with intuition).

**Remark 15.** *Recall the state decomposition in (29a) (which builds upon (20a) and (2)), and that  $\dot{\tilde{z}} = A\tilde{z}$ , for the linearized motion around the equilibrium. Then (for brevity, denote  $p = (x, y, z)$  and  $n = (\cdot, \psi, \theta)$ )*

$$\begin{bmatrix} P_x^T z \\ P_\delta^T z \\ P_y^T z \\ P_\psi^T z \end{bmatrix} = \begin{bmatrix} (x^{(0)}, x^{(1)}, x^{(2)}, x^{(3)}, x^{(4)}) \\ (\delta^{(0)}, \delta^{(1)}, \delta^{(2)}) |_{\delta=e_1^T(p_1-p_2)} \\ (y^{(0)}, y^{(1)}, y^{(2)}, y^{(3)}, y^{(4)}) \\ (\psi^{(0)}, \psi^{(1)}, \psi^{(2)}, \psi^{(3)}, \psi^{(4)}) \end{bmatrix}, \quad (54)$$

and (the equalities below can only be verified under an appropriate coordinate transformation – see [31, 36])

$$\begin{bmatrix} P_z^T z \\ P_\theta^T \theta \end{bmatrix} = \begin{bmatrix} (z^{(-1)}, z^{(0)}, z^{(1)}) \\ (\theta^{(-1)}, \theta^{(0)}, \theta^{(1)}) \end{bmatrix}. \quad (55)$$

That is,  $P_x$  is associated with the longitudinal ( $x$ ) linear motion of the bar (fifth order system) and  $P_\delta$  is associated with the longitudinal linear motion between the UAVs (third order system);  $P_y$  is associated with the lateral ( $y$ ) linear motion of the bar (fifth order system) and  $P_\psi$  is associated with the lateral angular motion of the bar (fifth order system). And finally,  $P_z$  is associated with the vertical ( $z$ ) linear motion of the bar (third order system) and  $P_\theta$  is associated with the vertical angular motion of the bar (third order system): to be specific, the sum of the integral errors is associated with the vertical linear position of the bar, and the difference is associated with the vertical angular position of the bar.

Given the state matrix  $A$  in (51) and the change of basis  $P$  in (53), it then follows that

$$PAP^{-1} = \begin{bmatrix} A_z \oplus A_\theta \oplus A_x \oplus A_\delta \oplus A_y \oplus A_\psi & \star \\ 0_{8 \times 24} & -\lambda I_{8 \times 8} \end{bmatrix} \quad (56)$$

whose entries are listed in Table 1.

### 6.3.1. Longitudinal motion

The matrices  $A_x$  and  $A_\delta$  describe the linear and angular longitudinal motions and, it follows from (45c), that they are Hurwitz provided that

$$k_r > k_{p,x}/k_{d,x}. \quad (57a)$$

i.e., provided that the attitude inner-loop gain is big enough. Since  $P_x z = e_1^T p =: x$  and  $P_\delta z = e_1^T (p_1 - p_2) =: \delta$ , it follows from (56) that, for the linearized motion, the bar's  $x$ -position behaves as a fifth-order integrator and the longitudinal displacement between UAVs behaves as a third-order integrator, i.e.,

$$\begin{aligned} x^{(5)}(t) &= (A_x)_{5,5} x^{(4)}(t) + \dots + (A_x)_{5,1} x^{(0)}(t), \\ \delta^{(3)}(t) &= (A_\delta)_{3,3} \delta^{(2)}(t) + \dots + (A_\delta)_{3,1} \delta^{(0)}(t). \end{aligned}$$

**Remark 16.** The linearized behaviour of the UAVs-bar system can be compared to that of a linearized container-crane system, where the goal is to stabilize the position of the container at the origin. Indeed, it follows that the linearized longitudinal ( $x$ ) linear motion of the bar is exactly that of the container in a container-crane system, with a cable of length  $l$ , being pulled by a crane of mass  $2M$ , and with a motor constant  $k_r$  [36].

### 6.3.2. Lateral motion

The matrices  $A_y$  and  $A_\psi$  describe the linear and angular lateral motions and, it follows from (45c), that they are Hurwitz provided that

$$k_r > k_{p,y}/k_{d,y}, \quad (58a)$$

i.e., provided that the attitude inner-loop gain is big enough. Since  $P_y z = e_2^T p =: y$  and  $P_\psi z = e_2^T n =: \psi$ , it follows

from (56) that, for the linearized motion, the bar's lateral linear motion and the bar's lateral angular motion behave as fifth-order integrators, i.e.,

$$\begin{aligned} y^{(5)}(t) &= (A_y)_{5,5} y^{(4)}(t) + \dots + (A_y)_{5,1} y^{(0)}(t), \\ \psi^{(5)}(t) &= (A_\psi)_{5,5} \psi^{(4)}(t) + \dots + (A_\psi)_{5,1} \psi^{(0)}(t). \end{aligned}$$

**Remark 17.** A similar remark to Remark 16 can be made at this point, regarding the lateral motions.

### 6.3.3. Vertical motion

The matrices  $A_z$  and  $A_\theta$  describe the linear and angular vertical motions and, it follows from (44), that they are both Hurwitz provided that

$$k_{i,z} < \min(\gamma_z, \gamma_\theta) k_{p,z} k_{d,z}. \quad (59a)$$

i.e., provided that the integral gain is *small enough*. Note that, for a standard PID (i.e.,  $\dot{x} = C_3(-(k_i, k_p, k_d)x)$ ), it is required that  $k_{i,z} < k_{p,z} k_{d,z}$ , while the constraint above is more restrictive, since  $\gamma_z < 1$  and  $\gamma_\theta < 1$  (see Table 1). Moreover, notice that  $\gamma_\theta$  vanishes when  $d$  vanishes (the distance of the contact points to the bar's center-of-mass): as such, it is advisable to have a *big*  $d$  (*big* compared to  $\sqrt{\frac{J}{2M}}$ ), because  $\gamma_\theta$  is closer to 1 (and thus the bound on the integral gain is less restrictive). This also agrees with intuition, which suggests that controlling the bar's attitude when the contact points are too close to the bar's center-of-mass is difficult. Under an appropriate coordinate change (see [31] or [36]), it can be verified that the sum of the integral errors is related to the vertical linear position of the bar (i.e., if  $z^{(-1)} \equiv \frac{d_2 \xi_{1,z} - d_1 \xi_{2,z}}{d_2 - d_1}$

then  $z^{(1)} \equiv \frac{d^2}{dt^2} \frac{d_2 \xi_{1,z} - d_1 \xi_{2,z}}{d_2 - d_1} = v_z$ ), while the difference between the integral errors is related to the vertical angular position of the bar (i.e., if  $\theta^{(-1)} \equiv \frac{\xi_{1,z} - \xi_{2,z}}{d_2 - d_1}$  then  $\theta^{(1)} \equiv \frac{d^2}{dt^2} \frac{\xi_{1,z} - \xi_{2,z}}{d_2 - d_1} = \omega_y$ ). As such, for the linearized motion,

$$\begin{aligned} z^{(2)}(t) &= (A_z)_{3,3} z^{(1)}(t) + (A_z)_{3,2} z^{(0)}(t) + (A_z)_{3,1} z^{(-1)}(t), \\ \theta^{(2)}(t) &= (A_\theta)_{3,3} \theta^{(1)}(t) + (A_\theta)_{3,2} \theta^{(0)}(t) + (A_\theta)_{3,1} \theta^{(-1)}(t). \end{aligned}$$

**Remark 18.** We also emphasize that, for the linearized motion, and for  $h \in \{x, y, z\}$ , the proportional and derivative gains  $k_{p,h}$  and  $k_{d,h}$  have an effect on the  $h$ -motion only, which agrees with intuition. This is however not the case when the bar is required to be under normal stress ( $F_* \neq 0$ ) nor when the bar is required to have a non-zero pitch ( $\theta_* \neq 0$ ) – see Sections 6.5 and 6.6.

**Remark 19.** The attitude gains of the vehicles do not play a role in the linearized vertical motion.

At this point, we defer the presentation of our main result (Theorem 24) till the end on the next subsection, which considers the generic case where the system is asymmetric.

### 6.4. Asymmetric UAVs-bar system

Let us now consider the case where the system is not symmetric, i.e., a system which does not satisfy the conditions in (70) (we assume only that  $d_1, d_2$  have opposite

signs – see Remark 3). The idea will be to choose the UAVs' gains so as to compensate for the asymmetries, in such a way that, if the system degenerates into a symmetric one, then the results of the previous section are recovered.

Consider again the similarity matrix  $P \in \mathbb{R}^{32 \times 32}$  as defined in (53) (which will be different than the  $P$  obtained in the previous section, which relied on the symmetry conditions), and whose determinant  $|P|$  is non-zero when  $d_1$  and  $d_2$  have opposite signs.

Given the state matrix  $A$  in (51) and the similarity matrix  $P$  in (53), it then follows that

$$PAP^{-1} = \begin{bmatrix} A_{z,\theta} \oplus A_{x,\delta} \oplus A_{y,\psi} & \star \\ 0_{8 \times 24} & -\lambda I_{8 \times 8} \end{bmatrix} \in \mathbb{R}^{32 \times 32}. \quad (60)$$

Similarly to the symmetric system, described in the previous section, there are three decoupled motions, namely a vertical, a longitudinal and a lateral. However, for the symmetric system, each of those motions was in turn composed of two decoupled sub-motions, one linear and one angular; that is not the case for the asymmetric system. The main idea explored next is to choose the control gains such that the linear sub-motion of the vertical/longitudinal/lateral motion is decoupled from the angular sub-motion. The difference with the case where the system is symmetric lies in that the linear and angular sub-motions are not decoupled. This will produce a state matrix that is similar to a block triangular matrix, which we are still able to analyze.

#### 6.4.1. Longitudinal motion

Recall Remark 15, and note that  $P_x$  and  $P_\delta$  are associated to  $A_{x,\delta} \in \mathbb{R}^{8 \times 8}$  in (60). As such,  $A_{x,\delta}$  is associated with the longitudinal motion, namely the longitudinal linear motion of the bar, and the longitudinal angular motion (corresponding to the longitudinal relative motion between the two UAVs). In what follows denote

$$F_x \equiv F_x(k_{p,x}^1, k_{p,x}^2, k_{d,x}^1, k_{d,x}^2, k_r^1, k_r^2) \in \mathbb{R}^3,$$

where  $F_x$  is some function of the gains shown above (found in the mathematica files in [36]). Note then that  $A_{x,\delta}$  has a specific structure, namely (below  $\star$  denotes a vector in  $\mathbb{R}^5$ )

$$A_{x,\delta} = \begin{bmatrix} A_x & e_5 F_x^T \\ e_3 \star^T & A_\delta \end{bmatrix} \in \mathbb{R}^{(5+3) \times (5+3)}. \quad (61)$$

Notice that  $A_{x,\delta}$  can be rendered block triangular, if one chooses the gains such that  $F_x$  in (61) vanishes. That is accomplished if the longitudinal gains are chosen as in (71), for some positive  $k_{p,x}$ ,  $k_{d,x}$ , and  $k_r$ . That is, the proportional and derivative gains of each vehicle must be the same up to some difference that is proportional to the asymmetry of the system, as quantified by  $\Delta_x$  described in (71). If the gains are chosen as in (71), then  $F_x = 0_3$  and  $A_{x,\delta}$  in (61) is block lower-triangular. The matrices  $A_x$  and  $A_\delta$  are those in Table 1, which are both Hurwitz provided that

$$k_r > k_{p,x}/k_{d,x}, \quad (62)$$

i.e., provided that the attitude inner-loop gain is big enough. This constraint can be comprehended intuitively: fast track-

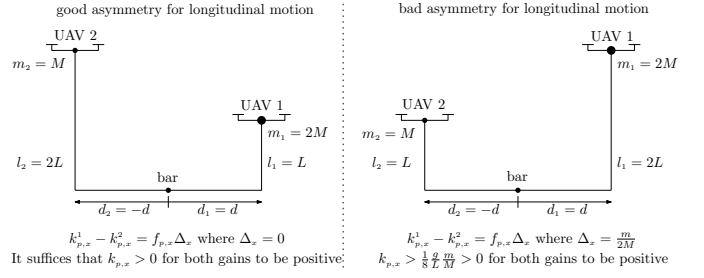


Figure 3: Good and bad asymmetries: it is better for the heavier UAV to be attached to the shorter cable as it minimizes  $|\Delta_x|$ . A good asymmetry only requires the gains  $k_{p,x}$ ,  $k_{d,x}$  to be positive, and a bad asymmetry requires both the proportional and the derivative gains to be strictly positive.

ing along the longitudinal direction requires a fast attitude inner-loop.

**Remark 20.** In (71), if one requires that  $k_{p,x}^1, k_{p,x}^2 > 0$ , then one must impose that  $k_{p,x} > -f_p \min \left( \frac{d_1 l_1 \Delta_x, d_2 l_2 \Delta_x}{d_1 l_1 - d_2 l_2} \right)$ , where  $\Delta_x$  encapsulates some measure of asymmetry of the system. As illustrated in Fig. 3, there are good and bad asymmetries: in good asymmetries  $\Delta_x = 0$  and, therefore, it is only required that  $k_{p,x}$  be positive; and, in bad asymmetries  $\Delta_x \neq 0$  and, therefore, it is required that  $k_{p,x}$  be strictly positive.

**Remark 21.** Recall Remark 15. It follows from (61) with  $F_x = 0_3$  that, for the linearized motion, (denote  $X := (x^{(0)}, \dots, x^{(4)})$  and  $\Delta := (\delta^{(0)}, \dots, \delta^{(2)})$ )

$$\begin{bmatrix} \dot{X} \\ \dot{\Delta} \end{bmatrix} = \begin{bmatrix} A_x & 0_{5 \times 3} \\ \star_{3 \times 5} & A_\delta \end{bmatrix} \begin{bmatrix} X \\ \Delta \end{bmatrix}, \quad (63)$$

i.e., the longitudinal linear motion behaves as a fifth order integrator and is decoupled from the longitudinal angular motion; while the longitudinal angular motion behaves as a third order integrator, cascaded after the longitudinal linear motion ( $A_x$  and  $A_\delta$  are those in Table 1).

**Remark 22.** Note that all parameters in Table 1 are positive, since  $d_1$  and  $d_2$  have opposite signs.

#### 6.4.2. Lateral motion

Recall Remark 15, and note that  $P_y$  and  $P_\psi$  are associated to  $A_{y,\psi} \in \mathbb{R}^{10 \times 10}$  in (60). As such,  $A_{y,\psi}$  is associated with the lateral motion, namely the lateral linear motion of the bar, and the lateral angular motion of the bar (yaw motion). In what follows denote

$$F_y \equiv F_y(k_{p,y}^1, k_{p,y}^2, k_{d,y}^1, k_{d,y}^2, k_{p,\psi}^1, k_{p,\psi}^2, k_{d,\psi}^1, k_{d,\psi}^2, k_r^1, k_r^2) \in \mathbb{R}^5,$$

where  $F_y$  is some function of the gains shown above (found in the mathematica files in [36]). Note then that  $A_{y,\psi}$  has a specific structure, namely

$$A_{y,\psi} = \begin{bmatrix} A_y & e_5 F_y^T \\ e_5 F_y^T & A_\psi \end{bmatrix} \in \mathbb{R}^{(5+5) \times (5+5)}. \quad (64)$$

Notice that  $A_{y,\psi}$  can be rendered block triangular, if one chooses the gains such that  $F_y$  in (64) vanishes (no choice of gains makes  $\tilde{F}_y$  vanish). That is accomplished if the

lateral gains are chosen as in (72), for some positive  $k_{p,y}$ ,  $k_{d,y}$ , and  $k_r$ . That is, the proportional and derivative gains of each vehicle must be the same up to some difference that is proportional to the asymmetry of the system, as quantified by  $\Delta_y$  (and  $|l_2 - l_1|$ ). If the gains are chosen as in (72), then  $F_y = 0_3$  and  $A_{y,\psi}$  in (64) is block lower-triangular. The matrices  $A_y$  and  $A_\psi$  are those in Table 1, which are both Hurwitz provided that

$$k_r > k_{p,y}/k_{d,y}, \quad (65)$$

i.e., provided that the attitude inner-loop gain is big enough. Note that similar remarks to Remarks 20, 21 and 22 can be made at this point regarding the lateral motion.

### 6.4.3. Vertical motion

Recall Remark 15, and note that  $P_z$  and  $P_\theta$  are associated to  $A_{z,\theta} \in \mathbb{R}^{6 \times 6}$  in (60). As such,  $A_{z,\theta}$  is associated with the vertical motion, namely the vertical linear motion of the bar, and the vertical angular motion of the bar (pitch motion).

In what follows denote

$$F_z \equiv F_z(k_{p,z}^1, k_{p,z}^2, k_{d,z}^1, k_{d,z}^2, k_{i,z}^1, k_{i,z}^2) \in \mathbb{R}^3,$$

where  $F_z$  is some function of the gains shown above. Note then that  $A_{z,\theta}$  has a specific structure, namely

$$A_{z,\theta} = \begin{bmatrix} A_z & e_3 F_z^T \\ e_3 F_z^T & A_\theta \end{bmatrix} \in \mathbb{R}^{(3+3) \times (3+3)}. \quad (66)$$

Notice that  $A_{z,\theta}$  can be rendered block triangular, if one chooses the gains such that either  $F_z$  or  $\tilde{F}_z$  in (66) vanish. We choose to cancel  $F_z$ , implying that we decouple the vertical-linear motion from the vertical-angular motion. That is accomplished if the vertical gains are chosen such that (73) is satisfied. That is, the proportional, derivative and integral gains of each vehicle must respect a ratio, which is exactly 1 under symmetry conditions (see (70)). In order to satisfy the conditions above, let, for  $h \in \{p, i, d\}$  and  $j \in \{1, 2\}$ ,

$$k_{h,z}^j = \frac{2\Delta_{z,j}}{\Delta_{z,1} + \Delta_{z,2}} k_{h,z}, \quad (67)$$

for some positive  $k_{p,z}$ ,  $k_{i,z}$ , and  $k_{d,z}$ , and with  $\Delta_{z,1}, \Delta_{z,2}$  as defined in (73)<sup>5</sup>. If the gains are chosen as in (67), then  $F_z = 0_3$  and  $A_{z,\theta}$  in (66) is block lower-triangular. The matrices  $A_z$  and  $A_\theta$  are those in Table 1, which are both Hurwitz provided that  $(\gamma_z, \gamma_\theta)$  are positive

$$k_{i,z} < \min(\gamma_z, \gamma_\theta) k_{p,z} k_{d,z}, \quad (68)$$

i.e., provided that the integral gain is *small enough*. Note that, for a standard PID, it is required that  $k_{i,z} < k_{p,z} k_{d,z}$ , while the constraint above is more restrictive, since  $\gamma_\theta < 1$ . Moreover, notice that  $\gamma_\theta$  vanishes when either  $d_1$  or  $d_2$  vanishes (the distance of the contact points to the bar's center-of-mass): as such, it is advisable to have a *large*  $|d_1|$  and  $|d_2|$  (*large* in the sense that  $\frac{J(d_1 m_1 - d_2 m_2)}{(-d_1 d_2) m_1 m_2 (d_1 - d_2)} \ll 1$ ), because  $\gamma_\theta$  is closer to 1 (and thus the bound on the integral gain is less restrictive). This also agrees with intuition,

which suggests that controlling the bar's attitude when the contact points are *too close* to the bar's center-of-mass is difficult.

**Remark 23.** The coefficients  $\gamma_z$  and  $\gamma_\theta$  in Table 1 are positive since  $d_1$  and  $d_2$  have opposite signs. Also, the attitude gains of the vehicles do not play a role in the linearized vertical motion.

We can now present our main result.

**Theorem 24.** Consider the UAVs-bar system, with vector field in (21), the dynamic control law (37) whose internal (integral) states evolve as in (30b), and the resulting closed-loop vector field  $\tilde{Z}_\gamma^{cl}$  in (41). Consider also the equilibrium  $\tilde{z}_\gamma^{cl}$  in (34), and let the desired configuration be  $\gamma = \gamma_*$  with  $\theta_* = 0$  and  $F_* = 0$  (i.e., the bar is to be stabilized on the horizontal plane and under no normal stress). Let also  $d_1$  and  $d_2$  have opposite signs. Finally, let the longitudinal, lateral and vertical gains of the control laws be chosen as in (71), (72) and (73), respectively, and such that (i) the attitude gain is big enough, as quantified in (62) and (65); and such that (ii) the integral gain is small enough, as quantified in (68). It then follows that the equilibrium  $\tilde{z}_\gamma^{cl}$  is exponentially stable.

Our main result, in Theorem 24, states that pose stabilization of the bar is accomplished, provided that the UAVs-bar system starts in some neighborhood of the equilibrium. The experiments provided in [31, 32] provide insight into the region of attraction of the equilibrium; in particular, convergence to the equilibrium was verified after impulsive disturbances were applied on both the bar and the UAVs.

### 6.5. Bar with non-zero pitch

In this subsection, we study the effect of requiring the angular position of the bar to have a non-zero vertical component (non-zero pitch angle), i.e., when  $\gamma_*$  in (25b) is chosen with  $\theta_* \in (-\frac{\pi}{2}, \frac{\pi}{2})$  and  $F_* = 0$ . This equilibrium configuration corresponds to the bottom left configuration shown in Fig. 2. For this purpose, and for simplicity, we assume that the UAVs are fully-actuated, that the system is symmetric (as defined in (70)), and that no integral action is being used. Let us anticipate the results that follow, where we find out that the vertical angular motion is coupled with the longitudinal angular motion.

For this system, the Jacobian  $A = DZ_{\gamma_*}^{cl}(z_{\gamma_*}) \in \mathbb{R}^{24 \times 24}$  is computed, where  $Z_{\gamma_*}^{cl}(z) := Z(z, u_{\gamma_*}^{pd}(z))$ , with  $Z$  in (7b),  $z_\gamma$  in (17) and  $u_\gamma^{pd}$  in (26). We then compute the change of basis matrix  $P \in \mathbb{R}^{24 \times 24}$ , with entries listed in Table 2 (and where  $P_\perp := (Df(z_\gamma))^T \in \mathbb{R}^{24 \times 6}$  with  $f$  as defined in (4)), which renders the matrix  $PAP^{-1}$  in block triangular form (just like in (52)). We note that  $|P| = -\frac{2d^2 g^6 m^2 \cos^2(\theta_*)}{J^2 L^{10}}$  is non-zero since  $\theta_* \in (-\frac{\pi}{2}, \frac{\pi}{2})$ , which guarantees that  $P$  is indeed a change of coordinates.

The diagonal entries of the matrix  $PAP^{-1}$  are listed in Table 2, and it follows that there are 5 decoupled motions, and that all matrices are Hurwitz for all  $\theta_* \in (-\frac{\pi}{2}, \frac{\pi}{2})$ . Indeed, it follows that the vertical linear, the longitudinal

<sup>5</sup>  $\frac{\Delta_{z,1}}{\Delta_{z,2}} > 0$  because  $d_1, d_2$  have opposite signs.

linear, the lateral linear and the lateral angular motions are all decoupled. On the other hand, it follows from  $A_{\theta,\delta}$  that the vertical angular motion is coupled to the longitudinal angular motion when  $\theta_* \neq 0$ . This coupling is, nonetheless, not detrimental to the stability of the equilibrium configuration, as the matrix  $A_{\theta,\delta}$  is Hurwitz for all  $\theta_* \in (-\frac{\pi}{2}, \frac{\pi}{2})$ . However, this conclusion is only valid for fully actuated UAVs; for under-actuated UAVs or for UAVs with vertical integral action, stricter conditions on the allowed interval for  $\theta_*$  may be required.

### 6.6. Bar under non-zero normal force

In this subsection, we study the effect of requiring the bar to be under a non-zero normal force/stress, i.e., when  $\gamma_*$  in (25b) is chosen with  $\theta_* = 0$  and  $F_* = r \frac{mg}{2}$ , for some  $r \in \mathbb{R}$ . This equilibrium configuration corresponds to the top right configurations shown in Fig. 2. Recall that  $F_*$  is twice the normal stress exerted on the bar and, for that reason,  $r$  represents the ratio of the normal force exerted on the bar with respect to the bar's weight. In studying this scenario, and for simplicity, we assume that the UAVs are fully-actuated, that the system is symmetric (as defined in (70)), and that no integral action is being used. Let us anticipate the results that follow, where we find out that the vertical and longitudinal motions are coupled, and that requiring the bar to be under tension is more beneficial than requiring the bar to be under compression.

For this system, the Jacobian  $A = DZ_{\gamma_*}^{cl}(z_{\gamma_*}) \in \mathbb{R}^{24 \times 24}$  is computed, where  $Z_{\gamma_*}^{cl}(z) := Z(z, u_{\gamma_*}^{pd}(z))$ , with  $Z$  in (7b),  $z_{\gamma_*}$  in (17) and  $u_{\gamma_*}^{pd}$  in (26). We then compute the change of basis matrix  $P \in \mathbb{R}^{24 \times 24}$ , with entries listed in Table 3 (and where  $P_{\perp} := (Df(z_{\gamma_*}))^T \in \mathbb{R}^{24 \times 6}$  with  $f$  as defined in (4)), which renders the matrix  $PAP^{-1}$  in block triangular form (just like in (52)). We note that  $|P| = -\frac{2d^2 g^6 m^2 (1+r^2)^3}{J^2 L^{10}}$  is non-zero for any  $r \in \mathbb{R}$ , which guarantees that  $P$  is indeed a change of coordinates.

The diagonal entries of the matrix  $PAP^{-1}$  are listed in Table 3, and it follows that there are four decoupled motions. The point  $p = e_1 - d \frac{J}{d^2 m} r e_6$  in  $P_{p,\theta}$ , defined in Table 3, is special in the sense that its position, velocity, acceleration and jerk (i.e.,  $A^0 p$ ,  $A^1 p$ ,  $A^2 p$  and  $A^3 p$ ) do not depend on any controller gains; this in turn guarantees that the change of basis matrix  $P$  also does not depend on any controller gains<sup>6</sup>. It follows from the matrices listed in Table 3 that, when the bar is under normal force, the linear vertical motion is coupled with the angular longitudinal motion (where the coupling vanishes when  $r = 0$ ); the motion of the point  $p$  (which corresponds to the linear longitudinal motion when  $r = 0$ ) is coupled with the angular vertical motion (where the coupling vanishes when  $r = 0$ ); where the only influence of the normal force in the linear lateral motion is to increase the frequency  $f_{p,y}$  ( $A_y$  in Table 3 is Hurwitz regardless of  $r$ ); and, finally, where the lateral angular motion is significantly influenced by the

normal force, i.e.,  $A_{\psi}$  in Table 3 is Hurwitz iff (note that  $q_{\psi}(1 - \tilde{q}_{\psi}) = \frac{J}{d^2 m} \frac{m}{2M} \frac{1}{\delta^2} > 0$ , as required by (46b))

$$k_{p,y} > -f_{p,\psi} q_{\psi} \tilde{q}_{\psi} = -\frac{g}{l} \frac{m}{2M} \frac{l}{d} r \left(1 + \frac{l}{d} \frac{r}{\sqrt{1+r^2}}\right)^{-1}. \quad (69)$$

This result confirms our intuition (next, and w.l.o.g., we assume that  $d > 0$ ). For simplicity, let  $d > l$ . Then, when we want the bar to be under tension ( $r > 0$ ), it suffices for the proportional gain  $k_{p,y}$  to be positive; on the other hand, when we want the bar to be under compression ( $r < 0$ ), the proportional gain  $k_{p,y}$  needs to be strictly positive (and arbitrarily large, if  $|r|$  is arbitrarily large). As such, one can say that requiring the bar to be under compression is less stable than requiring the bar to be under tension, because a bar under tension tends to restore the yaw position of the bar, while a bar under compression tends to destabilize the yaw position of the bar. This conclusion confirms the comments drawn during the analysis of the open-loop equilibria (see discussion after Proposition 4).

**Remark 25.** If  $d < l$  then the UAVs can cross paths, and there are three scenarios: when we want the bar to be under tension ( $r > 0$ ), it suffices for the proportional gain  $k_{p,y}$  to be positive; when we want the bar to be under mild compression ( $-\frac{d}{\sqrt{l^2-d^2}} < r < 0$ ), the proportional gain  $k_{p,y}$  needs to be strictly positive, and infinitely large as  $r$  approaches  $-\frac{d}{\sqrt{l^2-d^2}}$  (when  $r = -\frac{d}{\sqrt{l^2-d^2}}$ , then  $p_{1,\gamma} = p_{2,\gamma}$ , which corresponds to a scenario where the UAVs overlap); finally, when we want the bar to be under strong compression ( $r < -\frac{d}{\sqrt{l^2-d^2}}$ ), then, once again, it suffices that the proportional gain  $k_{p,y}$  be positive.

**Remark 26.** Notice that  $A_{z,\delta}$  and  $A_{p,\theta}$  are Hurwitz when  $r = 0$ , and, by continuity of the eigenvalues of a matrix, we can conclude that there is a neighborhood around 0, such that those matrices remain Hurwitz when  $r$  is in that neighborhood (that is, for a bar under some small tension or small compression, the matrices remain Hurwitz).

## 7. Experimental Results

We experimented the proposed control laws for a symmetric and an asymmetric system. The symmetric system is that illustrated in Fig. 1b, and the asymmetric is that illustrated in Fig. 1c. A video of the experiments is found at [youtu.be/ywwPvZuVpF0](https://youtu.be/ywwPvZuVpF0) and at [youtu.be/rgweowQ8fAE](https://youtu.be/rgweowQ8fAE), and a detailed description of the corresponding experimental results is found in [31, 32].

## 8. Conclusions

We proposed a control law for pose stabilization of a bar-cargo tethered to two UAVs. We modeled the system via a Newtonian approach, where we exploited the fact that the cables, connecting the bar to the UAVs, constrain the motion of the system to a manifold. We closed the loop with a saturated PID-like control law, for which one can guarantee that physical input limitations of each

<sup>6</sup>In particular, when  $r = 0$ , then  $p = e_1$  which corresponds to the longitudinal linear position of the bar.

UAV are respected. Finally, we provided conditions on the PID gains that guarantee that pose stabilization is accomplished; we described good and bad types of asymmetries; and we inferred that requiring the bar-cargo to be under tension is better for stability, as opposed to requiring the bar-cargo to be under compression.

- [1] AEROWORKS aim. <http://www.aeroworks2020.eu/>. (accessed April, 2018).
- [2] Q. Jiang and V. Kumar. The inverse kinematics of cooperative transport with multiple aerial robots. *IEEE Transactions on Robotics*, 29(1):136–145, Feb 2013.
- [3] M. Tognon, S. S. Dash, and A. Franchi. Observer-based control of position and tension for an aerial robot tethered to a moving platform. *IEEE Robotics and Automation Letters*, 1(2):732–737, July 2016.
- [4] Marco M. Nicotra, Roberto Naldi, and Emanuele Garone. Non-linear control of a tethered UAV: The taut cable case. *Automatica*, 78:174 – 184, 2017.
- [5] G. Schmidt and R. Swik. Automatic hover control of an unmanned tethered rotorplatform. *Automatica*, 10(4):393 – 403, 1974.
- [6] P. E. I. Pounds and A. M. Dollar. Stability of helicopters in compliant contact under PD-PID control. *IEEE Transactions on Robotics*, 30(6):1472–1486, Dec 2014.
- [7] P. J. Cruz, M. Oishi, and R. Fierro. Lift of a cable-suspended load by a quadrotor: A hybrid system approach. In *American Control Conference*, pages 1887–1892, July 2015.
- [8] Lorenzo Marconi, Roberto Naldi, and Luca Gentili. Modelling and control of a flying robot interacting with the environment. *Automatica*, 47(12):2571 – 2583, 2011.
- [9] A. Suarez, G. Heredia, and A. Ollero. Lightweight compliant arm with compliant finger for aerial manipulation and inspection. In *IEEE/RSJ International Conference on Intelligent Robots and Systems*, pages 4449–4454, Oct 2016.
- [10] C. Korpela, M. Orsag, M. Pekala, and P. Oh. Dynamic stability of a mobile manipulating unmanned aerial vehicle. In *International Conference on Robotics and Automation*, pages 4922–4927, 2013.
- [11] Hai-Nguyen Nguyen, ChangSu Ha, and Dongjun Lee. Mechanics, control and internal dynamics of quadrotor tool operation. *Automatica*, 61:289 – 301, 2015.
- [12] I. Palunko, P. Cruz, and R. Fierro. Agile load transportation: Safe and efficient load manipulation with aerial robots. *IEEE Robotics Automation Magazine*, 19(3):69–79, Sept 2012.
- [13] S. Tang and V. Kumar. Mixed integer quadratic program trajectory generation for a quadrotor with a cable-suspended payload. In *IEEE International Conference on Robotics and Automation*, pages 2216–2222, May 2015.
- [14] M. Tognon and A. Franchi. Dynamics, control, and estimation for aerial robots tethered by cables or bars. *IEEE Transactions on Robotics*, 33(4):834–845, Aug 2017.
- [15] S. J. Lee and H. J. Kim. Autonomous swing-angle estimation for stable slung-load flight of multi-rotor UAVs. In *IEEE International Conference on Robotics and Automation*, pages 4576–4581, May 2017.
- [16] Morten Bisgaard, Anders la Cour-Harbo, and Jan Dimon Bendtsen. Adaptive control system for autonomous helicopter slung load operations. *Control Engineering Practice*, 18(7):800 – 811, 2010. Special Issue on Aerial Robotics.
- [17] Shicong Dai, Taeyoung Lee, and Dennis S Bernstein. Adaptive control of a quadrotor UAV transporting a cable-suspended load with unknown mass. In *IEEE 53rd Annual Conference on Decision and Control*, pages 6149–6154. IEEE, 2014.
- [18] F. A. Goodarzi and T. Lee. Dynamics and control of quadrotor UAVs transporting a rigid body connected via flexible cables. In *American Control Conference*, pages 4677–4682, July 2015.
- [19] T. Lee, K. Sreenath, and V. Kumar. Geometric control of cooperating multiple quadrotor UAVs with a suspended payload. In *IEEE 52nd Annual Conference on Decision and Control*, pages 5510–5515, Dec 2013.
- [20] Konstantin Kondak, Markus Bernard, Fernando Caballero, Ivan Maza, and Anibal Ollero. Cooperative autonomous helicopters for load transportation and environment perception. *Advances in Robotics Research*, pages 299–310, 2009.
- [21] P. O. Pereira and D. V. Dimarogonas. Control framework for slung load transportation with two aerial vehicles. In *IEEE 56th Annual Conference on Decision and Control*, pages 4254–4259, Dec 2017.
- [22] T. Lee. Collision avoidance for quadrotor UAVs transporting a payload via voronoi tessellation. In *American Control Conference*, pages 1842–1848, July 2015.
- [23] P. O. Pereira and D. V. Dimarogonas. Nonlinear pose tracking controller for bar tethered to two aerial vehicles with bounded linear and angular accelerations. In *IEEE 56th Annual Conference on Decision and Control*, pages 4260–4265, Dec 2017.
- [24] T. Lee. Geometric control of multiple quadrotor UAVs transporting a cable-suspended rigid body. In *IEEE 53rd Annual Conference on Decision and Control*, pages 6155–6160, 2014.
- [25] Nathan Michael, Jonathan Fink, and Vijay Kumar. Cooperative manipulation and transportation with aerial robots. *Autonomous Robots*, 30(1):73–86, 2011.
- [26] M. Gassner, T. Cieslewski, and D. Scaramuzza. Dynamic collaboration without communication: Vision-based cable-suspended load transport with two quadrotors. In *IEEE International Conference on Robotics and Automation*, pages 5196–5202, May 2017.
- [27] H. Lee, H. Kim, and H. J. Kim. Planning and control for collision-free cooperative aerial transportation. *IEEE Transactions on Automation Science and Engineering*, PP(99):1–13, 2017.
- [28] S. Kim, S. Choi, H. Lee, and H. J. Kim. Vision-based collaborative lifting using quadrotor UAVs. In *14th International Conference on Control, Automation and Systems*, pages 1169–1174, Oct 2014.
- [29] M. Mohammadi, A. Franchi, D. Barcelli, and D. Prattichizzo. Cooperative aerial tele-manipulation with haptic feedback. In *IEEE/RSJ International Conference on Intelligent Robots and Systems*, pages 5092–5098, Oct 2016.
- [30] C. Masone, H. H. Bühlhoff, and P. Stegagno. Cooperative transportation of a payload using quadrotors: A reconfigurable cable-driven parallel robot. In *IEEE/RSJ International Conference on Intelligent Robots and Systems*, pages 1623–1630, Oct 2016.
- [31] P. O. Pereira and D. V. Dimarogonas. Collaborative transportation of a bar by two aerial vehicles with attitude inner loop and experimental validation. In *IEEE 56th Annual Conference on Decision and Control*, pages 1815–1820, Dec 2017.
- [32] P. O. Pereira, P. Roque, and D. V. Dimarogonas. Asymmetric collaborative bar stabilization tethered to two heterogeneous aerial vehicles. In *2018 IEEE International Conference on Robotics and Automation*, 2018 (to appear).
- [33] A. Tagliabue, M. Kamel, S. Verling, R. Siegwart, and J. Nieto. Collaborative transportation using MAVs via passive force control. In *IEEE International Conference on Robotics and Automation*, pages 5766–5773, May 2017.
- [34] P. O. Pereira and D. V. Dimarogonas. Stability of load lifting by a quadrotor under attitude control delay. In *IEEE International Conference on Robotics and Automation*, pages 3287–3292, May 2017.
- [35] M. Orsag, C. Korpela, M. Pekala, and P. Oh. Stability control in aerial manipulation. In *American Control Conference*, pages 5581–5586, June 2013.
- [36] P. O. Pereira and D. V. Dimarogonas. Mathematica files used in obtaining the manuscript’s results with a companion extended paper version. In <https://github.com/KTH-SML/pose-stabilization-of-bar-tethered-to-two-uavs.git>, 2018.
- [37] Jorge Cortés Monforte. *Geometric Control and Numerical Aspects of Nonholonomic Systems*. Springer-Verlag, 2002.
- [38] R. C. Nelson. *Flight Stability and Automatic Control*, volume 2. WCB/McGraw Hill, 1998.



Change of basis	Decoupled state matrices	Parameters when (70) holds	Parameters
$P_x := [e_1 \quad Ae_1 \quad A^3e_1 \quad A^4e_1]$	$A_x = \Gamma_5(q_x, (f_{p,x}, k_r), (k_{p,x}, k_{d,x}))$	$f_{p,x} = \frac{q}{l}, q_x = \frac{m}{2M}$	$f_{p,x} = \frac{g(d_1l_1-d_2l_2)}{l_1l_2(d_1-d_2)}, q_x = \frac{m(d_{11}^2m_1+d_{22}^2m_2)}{m_1m_2(d_1l_1-d_2l_2)^2}$
$P_\delta := [\nu \quad A\nu \quad A^2\nu] \big _{\nu=e_7-e_{10}}$	$A_\delta = \Gamma_3(\tilde{f}_{p,x}, (k_{p,x}, k_{d,x}))$	$\tilde{f}_{p,x} = \frac{q}{l} \frac{m}{2M}$	$\tilde{f}_{p,x} = \frac{gm(d_{11}^2m_1+d_{22}^2m_2)}{l_1l_2m_1m_2(d_1-d_2)(d_1l_1-d_2l_2)}$
$P_y := [e_2 \quad Ae_2 \quad A^3e_2 \quad A^4e_2]$	$A_y = \Gamma_5(q_y, (f_{p,y}, k_r), (k_{p,y}, k_{d,y}))$	$f_{p,y} = \frac{q}{l}, q_y = \frac{m}{2M}$	$f_{p,y} = \frac{g(d_1l_1-d_2l_2)}{l_1l_2(d_1-d_2)}, q_y = \frac{m(d_{11}^2m_1+d_{22}^2m_2)}{m_1m_2(d_1l_1-d_2l_2)^2} + \frac{-md_1d_2-d_1d_2(l_1-l_2)^2}{j(d_1l_1-d_2l_2)^2}$
$P_\psi := [e_5 \quad Ae_5 \quad A^2e_5 \quad A^4e_5]$	$A_\psi = \Gamma_5(q_\psi, (f_{p,\psi}, k_r), (k_{p,\psi}, k_{d,\psi}))$	$f_{p,\psi} = \frac{d^2m}{j} f_{p,y}, q_\psi = \frac{j}{d^2m} q_y$	$f_{p,\psi} = \frac{-md_1d_2}{j} f_{p,y}, q_\psi = \frac{j}{-md_1d_2} q_y$
$P_z := [\nu \quad A\nu \quad A^2\nu] \big _{\nu=\frac{d_2e_{31}-d_1e_{32}}{d_2-d_1}}$	$A_z = C(\gamma_z(k_{i,z}, k_{p,z}, k_{d,z}))$	$\gamma_z = \left(1 + \frac{m}{2M}\right)^{-1}$	$\gamma_z = \gamma_\theta \frac{\Delta_{z,2}}{\Delta_{z,1}\Delta_{z,2}} \frac{1}{m(d_{11}^2m_1+d_{22}^2m_2)^2} \frac{1}{1+\frac{m(m+m_1+m_2)}{(d_1-d_2)^2m_1m_2}}$   see (73)
$P_\theta := [\nu \quad A\nu \quad A^2\nu] \big _{\nu=\frac{e_{31}-e_{32}}{d_2-d_1}}$	$A_\theta = C(\gamma_\theta(k_{i,z}, k_{p,z}, k_{d,z}))$	$\gamma_\theta = \left(1 + \frac{j}{d^2m} \frac{m}{2M}\right)^{-1}$	$\gamma_\theta = \left(1 + \frac{j(d_1m_1-d_2m_2)}{2(-d_1d_2)m_1m_2(d_1-d_2)}\right)^{-1}$

Table 1: Decoupled state matrices with  $\theta_\star = 0$  and  $F_\star = 0$  (no pitch and no normal force). Matrices  $\Gamma_5$ ,  $C_3$  defined in Section 5.

Change of basis	Decoupled state matrices	Parameters
$P_z := [e_3 \quad Ae_3]$	$A_z = C_2(\gamma_z(k_{p,z}, k_{d,z}))$	$\gamma_z = \left(1 + \frac{m}{2M}\right)^{-1}$
$P_{\theta,\delta} := [e_6 \quad Ae_6 \quad \nu \quad A\nu] \mid \nu = e_T - e_{10}$	$A_{\theta,\delta} = \begin{bmatrix} C_2(-\gamma_\theta(k_{p,z} + \tan(\theta_\star)^2 f_{p,x}, k_{d,z})) & -\frac{f_{p,x}}{2d} \gamma_\theta \tan(\theta_\star) e_2 e_1^T \\ -2d \tan(\theta_\star) f_{p,x} e_2 e_1^T & C_2(-(k_{p,x} + f_{p,x} k_{d,x})) \end{bmatrix}$	$\gamma_\theta = \left(1 + \frac{J}{d^2 m} \frac{m}{2M} \frac{1}{\cos(\theta_\star)^2}\right)^{-1}, f_{p,x} = \frac{g}{l} \frac{m}{2M}$
$P_x := [e_1 \quad Ae_1 \quad A^2 e_1 \quad A^3 e_1]$	$A_x = \Gamma_4(q_x, f = (f_{p,x}, k_r), (k_{p,x}, k_{d,x}))$	$f_{p,x} = \frac{g}{l}, q_x = \frac{m}{2M}$
$P_y := [e_2 \quad Ae_2 \quad A^2 e_2 \quad A^3 e_2]$	$A_y = \Gamma_4(q_y, f_{p,y}, k = (k_{p,y}, k_{d,y}))$	$f_{p,y} = \frac{g}{l}, q_y = \frac{m}{2M}$
$P_\psi := [e_5 \quad Ae_5 \quad A^2 e_5 \quad A^3 e_5]$	$A_\psi = \Gamma_4(q_\psi, f_{p,\psi}, k = (k_{p,y}, k_{d,y}))$	$f_{p,\psi} = \frac{J}{d^2 m} f_{p,y}, q_\psi = \frac{J}{d^2 m} q_y$

Table 2: Decoupled state matrices when bar is required to have non-zero pitch angle  $\theta_*$ . Matrices  $\Gamma_4$ ,  $C_2$  defined in Section 5.

$$l_1 = l_2 =: l > 0, d_1 = -d_2 =: d \in \mathbb{R}, m_1 = m_2 =: m > 0, k_{l,h}^1 = k_{l,h}^2 =: k_r^j > 0, k_{p,\psi}^j = 0, k_{d,\psi}^j = 0. \quad (70)$$

$$F_x = 0_3 \Leftrightarrow k_{p,x}^j = k_{p,x}^j + \frac{d_{l_j}}{d_{l_1} - d_{l_2}} f_{p,x} \Delta_x^j = k_{d,x}^j + \frac{d_{l_j}}{d_{l_1} - d_{l_2}} f_{p,x} \Delta_x^j = k_r^j = k_r^j = k_r^j, \Delta_x = \frac{m(d_{l_1} m_1 + d_{l_2} m_2)}{m \cdot m_2 (d_{l_1} - d_{l_2})}, \quad (71)$$

$$F_y = 0 \Leftrightarrow \begin{cases} k_{p,y}^j = k_{p,y}^* + \frac{d_{j,l_j} f_{p,y} \Delta_y}{d_{j,l_1} - d_{j,l_2}} \\ k_{d,y}^j = k_{d,y}^* + \frac{d_{j,l_j} f_{p,y} \Delta_y}{d_{j,l_1} - d_{j,l_2}} \end{cases}, \quad \begin{cases} k_{p,\psi}^j = \frac{d_{j,l_j}}{d_{j,l_1} - d_{j,l_2}} \left( \frac{d_{j,l_j}}{d_{j,l_1} - d_{j,l_2}} \frac{f_{p,y}}{k_r} \Delta_y + \frac{l_2 - l_1}{l_1 l_2} k_{p,y} \right) \\ k_{d,\psi}^j = \frac{d_{j,l_j}}{d_{j,l_1} - d_{j,l_2}} \left( \frac{d_{j,l_j}}{d_{j,l_1} - d_{j,l_2}} \frac{f_{p,y}}{k_r} \Delta_y + \frac{l_2 - l_1}{l_1 l_2} k_{d,y} \right) \end{cases}, \quad \begin{cases} k_r^1 = k_r^2 = k_r \\ \Delta_y = \frac{m(d_{j,l_1} m_1 + d_{j,l_2} m_2)}{m_1 m_2 (d_{j,l_1} - d_{j,l_2})} + \frac{-m d_{j,l_2} (d_{j,l_1} - l_2)}{j (d_{j,l_1} - d_{j,l_2})} \end{cases}, \quad (72)$$

$$F_z = 0_3 \Leftrightarrow \frac{k_{p,z}^1}{k_{p,z}^2} = \frac{k_{d,z}^1}{k_{d,z}^2} = \frac{k_{i,z}^1}{k_{i,z}^2} = \frac{-m_2 d_2 (J + d_1 m_1 (d_1 - d_2))}{+m_1 d_1 (J + d_2 m_2 (d_2 - d_1))} = \frac{\Delta_{z,1}}{\Delta_{z,2}}.$$

Change of basis	Decoupled state matrices	Parameters
$P_{z,\delta} := \begin{bmatrix} e_3 & Ae_3 \\ \nu & A\nu \end{bmatrix} \big _{\nu=e_7-e_{10}}$	$A_{z,\delta} = C_2(-\gamma_z(k_{p,z}, k_{d,z})) \oplus C_2(-(k_{p,x} + f_{p,x}, k_{d,x})) + \mathcal{O}( r )$	$\gamma_z = \left(1 + \frac{m}{2M}\right)^{-1}, f_{p,x} = \frac{g}{l} \frac{m}{2M}$
$P_{p,\theta} := \begin{bmatrix} e_6 & Ae_6 \\ p & Ap \end{bmatrix} A^2 p \quad A^3 p$	$A_{p,\theta} = C_2(-\gamma_\theta(k_{p,z}, k_{d,z})) \oplus \Gamma_4(q_x, f_{p,x}, (k_{p,x}, k_{d,x})) + \mathcal{O}( r )$	$\gamma_\theta = \left(1 + \frac{J}{d^2 m} \frac{m}{2M}\right)^{-1}, f_{p,x} = \frac{g}{l}, q_x = \frac{m}{2M}$
$P_y := \begin{bmatrix} e_2 & Ae_2 \\ A^2 e_2 & A^3 e_2 \end{bmatrix}$	$A_y = \Gamma_4(q_y, f_{p,y}, (k_{p,y}, k_{d,y}))$	$f_{p,y} = \frac{g}{l} \sqrt{1 + r^2}, q_y = \frac{m}{2M}$
$P_\psi := \begin{bmatrix} e_5 & Ae_5 \\ A^2 e_5 & A^3 e_5 \end{bmatrix}$	$A_\psi = \tilde{\Gamma}_4(\tilde{q}_\psi, q_\psi, f_{p,\psi}, (k_{p,\psi}, k_{d,y}))$	$f_{p,\psi} = \frac{d^2 m}{J} \delta f_{p,y}, q_\psi = \frac{J}{d^2 m} \delta^{-1} q_y, \tilde{q}_\psi = \frac{\delta^{-1}}{\delta}, \delta = \left(1 + \frac{l}{a} \frac{r}{\sqrt{1+r^2}}\right)$

Table 3: Decoupled state matrices when bar is required to be under a non-zero normal force  $F_*$  (where  $p = e_1 - d \frac{j}{d^{2-m}} re_6$ ). Matrices  $\Gamma_4, \bar{\Gamma}_4, C_2$  defined in Section 5.